DISCOVERY OF ENZYMES RESPONSIBLE FOR AN ALTERNATE MEVALONATE PATHWAY IN *HALOFERAX VOLCANII*

A DISSERTATION IN
Molecular Biology and Biochemistry
and
Cell Biology and Biophysics

Presented to the Faculty of the University
of Missouri-Kansas City in partial fulfillment of
the requirements for the degree

DOCTOR OF PHILOSOPHY

by
JOHN CURTIS VANNICE

M.S., University of Missouri - Kansas City, 2010
B.S., University of Kansas, Lawrence, 2003

Kansas City, Missouri
2014

DISCOVERY OF ENZYMES RESPONSIBLE FOR AN ALTERNATE MEVALONATE PATHWAY IN *HALOFERAX VOLCANII*

John Curtis VanNice, Candidate for the Doctor of Philosophy Degree

University of Missouri - Kansas City, 2014

ABSTRACT

Archaea are a distinct evolutionary domain of microorganisms that contain isoprenoids in ether linkages to glycerol rather than the ester linked fatty acids that characterize membranes of bacteria or eukaryotes. Radiolabeling experiments with acetate and mevalonate strongly implicate the mevalonate pathway in providing the isoprenoids for archaeal lipid biosynthesis. However, the enzymes responsible for mevalonate metabolism in archaea have remained either cryptic or poorly characterized. To identify the enzymes responsible for the mevalonate pathway in *Haloferax volcanii*, open-reading frames from the *H. volcanii* genome were candidate screened against bacterial and eukaryotic mevalonate pathway enzymes and overexpressed in a *Haloferax* host.

This approach has revealed that *H. volcanii* encodes (HVO_2419) a 3-hydroxy-3-methylglutaryl-CoA synthase (EC 2.3.310) which is the first committed step of the mevalonate pathway. Kinetic characterization shows that *H. volcanii* 3-hydroxy-3-methylglutaryl-CoA synthase (*Hv*HMGCS) exhibits substrate saturation and catalytic efficiency similar to known bacterial and eukaryotic forms of the enzyme. *Hv*HMGCS is unique in that it does not exhibit substrate inhibition by acetoacetyl-CoA. *Hv*HMGCS is

inhibited by hymeglusin, a specific inhibitor of bacterial and eukaryotic HMGCS, with experimentally determined K_i of 570 ± 120 nM and k_{inact} of 17 ± 3 min^{-1}. Hymeglusin also prevents the growth of *H. volcanii* cells *in vivo* suggesting the essentiality of the enzyme and the mevalonate pathway in these microbes.

H. volcanii also encodes (HVO_2762) an isopentenyl monophosphate kinase (EC 2.7.4.26) and a novel decarboxylase (HVO_1412) that has been proposed, but never demonstrated, to produce isopentenyl monophosphate. This enzyme uses phosphomevalonate and ATP as substrates while exhibiting negligible decarboxylase activity with either mevalonate or mevalonate diphosphate. Phosphomevalonate decarboxylase (PMD) exhibits an IC_{50} = 16 µM for 6-fluoromevalonate monophosphate but negligible inhibition by 6-fluoromevalonate diphosphate, reinforcing its selectivity for monophosphorylated ligands. Inhibition by the fluorinated analog also suggests that PMD utilizes the reaction mechanism that has been demonstrated for the classical mevalonate pathway decarboxylase. These observations mark the accomplishment of the identification of a novel phosphomevalonate decarboxylase in *H. volcanii*.

Identification and functional characterization of these enzymes also demonstrate, for the first time, the existence of the enzymes responsible for an alternate mevalonate pathway in *H. volcanii*.

The faculty listed below, appointed by the Dean of the School of Graduate Studies, have examined a dissertation titled "Discovery of Enzymes Responsible for an Alternate Mevalonate Pathway in *Haloferax volcanii*" presented by John C. VanNice, candidate for the Doctor of Philosophy degree, and certify that in their opinion it is worthy of acceptance.

Supervisory Committee

Henry M. Miziorko, Ph.D., Committee Chair
Department of Molecular Biology and Biochemistry

Brian V. Geisbrecht, Ph.D.
Department of Biochemistry and Molecular Biophysics,
Kansas State University

Gerald J. Wyckoff, Ph.D.
Department of Molecular Biology and Biochemistry

Samuel Bouyain, D.Phil.
Department of Molecular Biology and Biochemistry

William G. Gutheil, Ph.D.
Division of Pharmaceutical Sciences, School of Medicine,
University of Missouri-Kansas City,

CONTENTS

ILLUSTRATIONS

Figure Page

TABLES

Table Page

ABBREVIATIONS

ACN	acetonitrile
amp	ampicillin
ADP	adenosine 5’-diphosphate
ATP	adenosine 5’-triphosphate
C-terminus	carboxy-terminus
^{14}C	carbon 14
CHES	N-Cyclohexyl-2-aminoethanesulfonic acid
CDP-ME	4-diphosphocytidyl-2-C-methylerythritol
CDP-MEP	4-diphosphocytidyl-2-C-methyl-D-erythritol 2-phosphate
CoA	Coenzyme A
DMAPP	dimethylallylpyrophosphate
DMSO	dimethylsulfoxide
DOXP	1-Deoxy-D-xylulose 5-phosphate
DTT	dithiothreitol
DNA	deoxyribonucleic acid
EC	enzyme commission
E. faecalis	*Enterococcus faecalis*
E. coli	*Escherichia coli*
ε	extinction coefficient

g	gravity
GHMP	galatokinase/homoserine/mevalonate/ Phosphomevalonate
HMB-PP	4-Hydroxy-3-methyl-but-2-enylpyrophosphate
His-tag	Histidine tag
HMG-CoA	3-hydroxy-3-methyl-glutary-Coenzyme A
H. NRC-1	*Halobacterium NRC-1*
H. volcanii	*Haloferax volcanii*
hdrB	gene for dihydrofolate reductase
Hv-Ca	*Haloferax volcanii* – Casamino acids
Hv-YPC	*Haloferax volcanii* – Yeast Extract, Peptone, Casamino acids
IP	isopentenyl 5'-monophosphate
IPK	isopentenyl 5'-monophosphate kinase
IPP	isopentenyl 5'-pyrophosphate
k_{cat}	turnover number
kDa	kilodaltons
K_i	inhibition coefficient
K_m	Michaelis constant
KCl	potassium chloride
MeOH	methanol
$MgCl_2$	magnesium chloride

M	molar
mM	millimolar
µM	micromolar
nM	nanomolar
µM	microliter
Mg	magnesium
mg	milligram
mL	milliliter
mg/mL	milligram / milliliter
$M^{-1}cm^{-1}$	per molar per centimeter
MEcPP	2-C-methyl-D-erythritol 2,4-cyclopyrophosphate
MEP	2-C-methylerythritol 4-phosphate
MDD	mevalonate diphosphate decarboxylase
MVA	mevalonate
MVP	mevalonate 5-phosphate
MVPP	mevalonate 5-diphosphate
M. jannaschii	*Methanocaldococcus jannaschii*
M. maripaludis	*Methanococcus maripaludis*
M. smithii	*Methanobrevibacter smithii*
NaCl	sodium chloride
NADH	nicotinamide adenine dinucleotide, reduced

NAD+	nicotinamide adenine dinucleotide, oxidized
NADPH	nicotinamide adenine dinucleotide phosphate, Reduced
NADP+	nicotinamide adenine dinucleotide, phosphate oxidized
N-terminus	amino terminus
nm	nanometer
PCR	polymerase chain reaction
PMD	phosphomevalonate decarboxylase
PMK	phosphomevalonate kinase
pyrE2	gene for orotate phosphoribosyl transferase
SDS-PAGE	sodium dodecyl sulfate polyacrylamide gel electrophoresis
S. aureus	*Staphylococcus aureus*
S. pneumonia	*Streptococcus pneumonia*
S. solfataricus	*Sulfolobus solfataricus*
TRIS	tris(hydroxymethyl)aminomethane
U	unit, µmole min^{-1}
U/mg	unit/milligram, µmole $min^{-1}mg^{-1}$
V_{max}	maximum velocity

ACKNOWLEDGEMENTS

I would like to thank Dr. Henry Miziorko for providing me guidance and support throughout my time in graduate school. Dr. Miziorko was always there with advice but also willing to allow me to explore.

I would also like to thank my committee members Dr. Brian Geisbrecht, Dr. Gerald Wyckoff, Dr. Samuel Bouyain, and Dr. William Gutheil. Dr. Geisbrecht always reminded me to 'go cowboy' encouraging me to be bold with my work. Dr. Wyckoff will always remain my Gandalf in the Middle-Earth of evolution and bioinformatics. Dr. Bouyain and Dr. Gutheil provided invaluable advice on both my dissertation and the world of science as a whole.

There are also a number of people that deserve special recognition. I would like to thank Rana Zalmai and Chris Willig for their original work on isopentenyl monophosphate kinase and high-salt, ATP-utilizing coupling systems, respectively. The mass spectrometry work provided by Dr. Keightly was invaluable. I would like to thank Dr. Michael O'Connor for taking a chance on me and Dr. Karen Bame for her patient guidance in the grant writing class. Dr. Kasra Ramyar, Dr. Brandon Garcia, and Joe McWhorter deserve thanks for their advice and specifically for teaching me the art of sub-cloning. I would also like to thank all of the current and former members of the Miziorko lab. I stand on their shoulder in this endeavor.

I would also like to thank my parents, John and Christy VanNice, for their unwavering support. Finally, I would like to thank my darling wife and son, Kimberly and John Patrick. All my love.

CHAPTER 1

INTRODUCTION

Archaea are single-celled microorganisms that represent the Third Domain of Life. Phylogenetic analyses reveal that these microbes are one of the three direct lineages that emerged from the primordial world (1). The differences between these lineages were discovered to be so profound that it required a change in the biological classification system (2). Archaea are now positioned in a separate domain with bacteria and eukaryotes representing the other domains and creating the three domain biological classification system most prominent today. Their unique nature and independent evolutionary history prompts vigorous debate about not only the evolutionary path of all organisms but also the origin of life itself.

Investigation into the archaeal domain has revealed that these microbes are similar to bacteria in some respects, similar to eukaryotes in others- and in some cases decidedly unique. Archaea are morphologically similar to bacteria as both are single-celled and do not possess a nucleus or any other membrane bound organelles (3). Most archaea protect their cells by a cell wall of protein and glycoprotein as an S-layer similar to gram positive bacteria but do not use peptidoglycan in its synthesis (4). All archaea possess a circular DNA genome similar to bacteria but some wrap their genomic DNA around histones in a manner similar to eukaryotes (5). Archaeal histones lack the N- and C-terminal extensions utilized by eukaryotes for chromatin remodeling suggesting that archaea do no utilize this process (5,6). Information processing in archaea contains some similarities to both bacteria and

eukaryotes. Archaea organize similar open reading frames into operons and produce polycistronic mRNAs similar to bacteria (5). However, archaea utilize eukaryotic forms of RNA polymerase (7) and transcription factors (5). Archaeal transcription regulators are more similar to bacteria (8). Archaeal mRNA is not capped as in eukaryotes, frequently does not possess a Shine-Delgarno sequence seen in bacteria, and instead is often leaderless (9). The archaeal ribosome is made of a number of proteins that share homology to both bacteria and eukaryotes (5). Archaea are metabolically diverse and utilize a variety of sources of energy. The methanogens from domain Archaea are the only known organisms that use carbon dioxide as an electron acceptor to produce methane (10). Several archaea can use carbon dioxide as a source of carbon (10). Halophiles can use light to create chemical energy in the form of ATP (10). Some archaea can oxidize ammonia, fix nitrogen, and reduce sulfate, while others oxidize sulfur (4). Their metabolic diversity and abundant global biomass of 20% (11) suggest that archaea play lead roles in a number of global biogeochemical cycles (4).

Archaea are immediately recognized as a domain of extremophiles. Representatives of the archaeal domain can be found thriving in the harshest terrestrial environments. These ecological extremes comprise conditions of high pressure, extreme temperature, acidity, and salinity. Examples include *Methanocaldococcus jannaschii* which was isolated from an underwater volcanic thermal vent (12), *Sulfolobus solfataricus* found in a solfataric field and grows optimally at 80^{o}C and in high acidity (13), and *Haloferax volcanii* discovered in saturating levels of salt in the Dead Sea (14). Some other notable archaea are *Ferroplasma acidiphilum* which grows in high levels of iron and acid with 86% of their

proteome being iron metallo-proteins (15) and *Picrophilus torridus* which can grow in 1.2M acid (16). Another extreme archaea is *Methanopyrus kandleri* which has been observed growing at 122°C (17). While there are some examples of mesophilic archaea, these microbes are frequently obligate anaerobes. For instance, *Methanococcus maripaludis*, a methanogen isolated from a marsh habitat, requires dedicated anoxic facilities and techniques to culture (18). *Methanbrevibacter smithii*, another obligate anaerobe, is part of normal human flora inhabiting the human gastrointestinal tract aiding in the digestion of polysaccharides (19).

Along with their evolutionary history and extremophilic nature, archaea are unique in the structure and synthesis of their lipid membranes. Archaeal lipid membranes are characterized by a side-branching, phytanyl moiety. These lipids are synthesized from isopentenyl diphosphate, an isoprenoid, and are ether-linked to glycerol 1-phosphate (Fig 1) (20, 21). To produce the standard archaeal lipid, isopentenyl diphosphate (IPP) is first enzymatically isomerized to dimethylallyl diphosphate (DMAPP) by isopentenyl diphosphate isomerase. IPP and DMAPP then undergo chain elongation to form geranylgeranyl diphosphate (22). The final reaction is catalyzed by the multifunctional enzyme, geranylgeranyl diphosphate synthase (GGPS), to produce the polyisoprenoid lipid (23). Some diversity in archaea lipids has been noted. Chain length can vary by the inclusion of five carbons from additional IPP to produce C25 and even C40 lipids (24). Archaeal C40

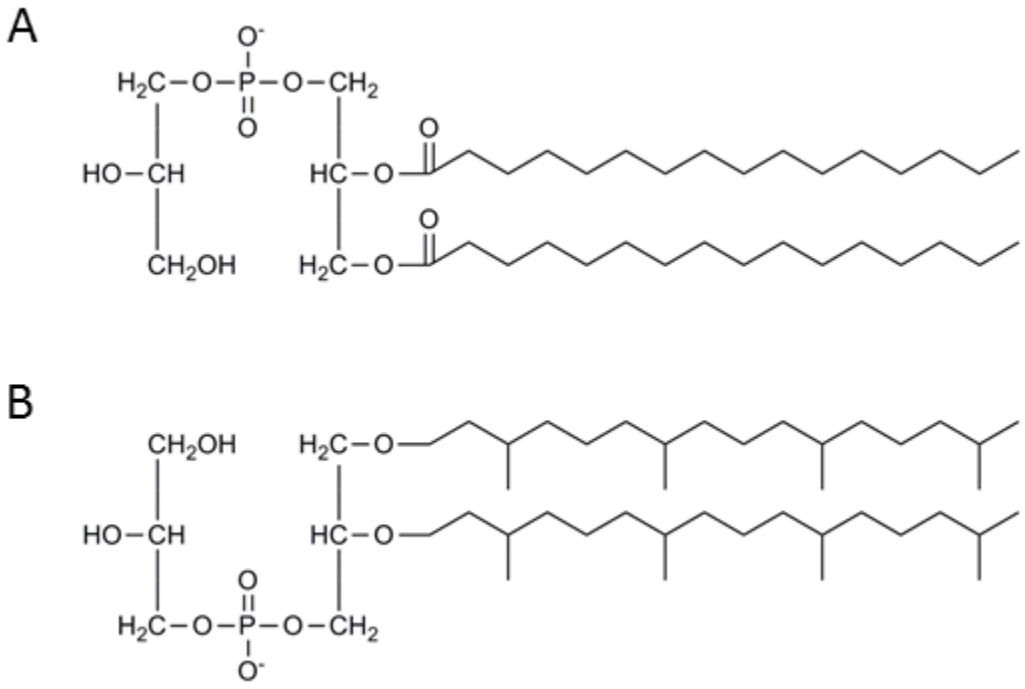

Figure 1. Bacterial, Eukaryotic, and Archaeal Phospholipid. The chemical structure of the phospholipid used in lipid membrane biosynthesis from bacteria, eukaryotes, and archaea. A) bacterial and eukaryotic lipids are characterized by fatty acids ester-linked to glycerol 3-phosphate B) archaeal phospholipids are characterized by polyisoprenoids ether-linked to glycerol 1-phosphate.

lipids have been observed as both cyclic archaeol or with the tails covalently-linked to produce tetraethers (25). Bacterial and eukaryotic lipid membranes, in contrast, are characterized by the utilization of fatty acids ester-linked to glycerol 3-phosphate (Fig 1). The most common bacterial and eukaryotic fatty acid, palmitic acid, is enzymatically synthesized in six recurring reactions starting with malonyl-CoA and acetyl-CoA. These reactions are catalyzed by the multifunctional, NADPH-dependent enzyme fatty acid synthase. There is some diversity in bacterial and eukaryotic lipids, as well. For instance, fatty acids can vary in chain length and saturation. However, each is generally produced by the inclusion of two carbons from acetyl-CoA.

The isoprenoid, isopentenyl diphosphate, is biologically synthesized by two pathways. Eukaryotes and some gram positive bacteria utilize the mevalonate pathway to produce isopentenyl diphosphate (26). The mevalonate pathway is characterized by the condensation of three acetyl-CoA molecules in a series of six reactions to produce isopentenyl diphosphate (Fig 2) (26). The first committed step, catalyzed by the enzyme 3-hydroxy-3-methylglutaryl-CoA synthase, condenses one molecule of acetyl-CoA and one molecule of acetoacetyl-CoA to produce 3-hydroxy-3-methylglutaryl-CoA (HMG-CoA). This step is physiologically irreversible and commits acetate to the mevalonate pathway. HMG-CoA is then reduced by the NAD(P)H -utilizing enzyme HMG-CoA reductase to produce mevalonic acid. The eukaryotic mevalonate pathway is regulated by HMG-CoA reductase and is also inhibited by statins that are widely used to lower cholesterol. Mevalonate kinase then phosphorylates mevalonic acid using ATP as the phosphoryl donor to produce mevalonate 5-phosphate which is then phosphorylated again

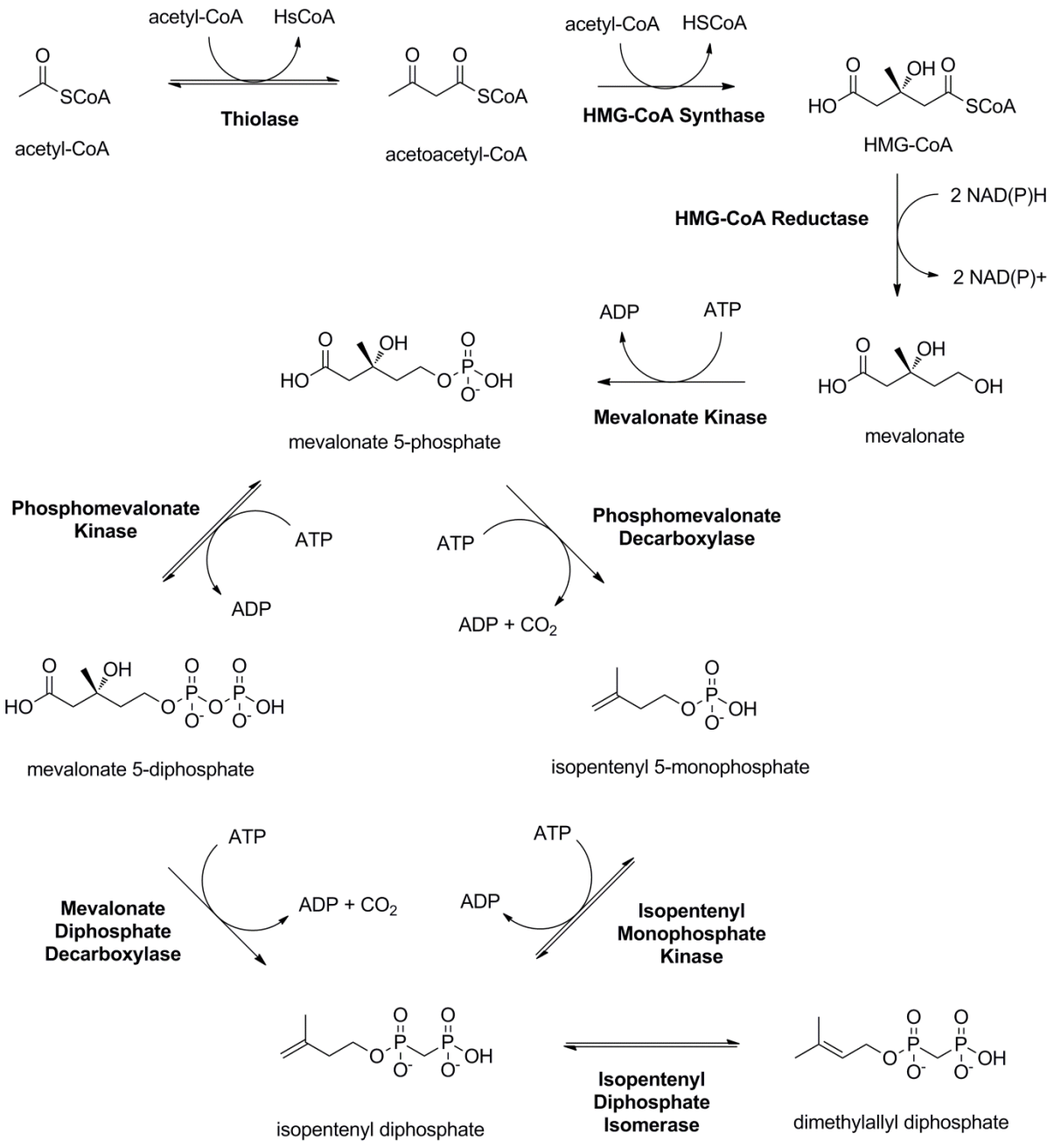

Figure 2. The Classical (left) and Proposed Alternate (right) Mevalonate Pathway.

Figure 2. Continued. The mevalonate pathway is responsible for the production of isopentenyl diphosphate from acetate. The enzymes of the classical and proposed alternate mevalonate pathway differ in the terminal reactions only. The classical mevalonate pathway is catalyzed by phosphomevalonate kinase and mevalonate diphosphate decarboxylase which is indicated on the left side of the diamond and the proposed alternate mevalonate pathway catalyzed by a putative phosphomevalonate decarboxylase and isopentenyl monophosphate kinase is indicated on the right.

in a reversible reaction by the enzyme phosphomevalonate kinase using ATP to produce mevalonate 5-diphosphate. Mevalonate 5-diphosphate is then decarboxylated by the ATP-utilizing enzyme mevalonate diphosphate decarboxylase to produce isopentenyl-diphosphate. Isopentenyl-diphosphate is then isomerized to dimethylallyl diphosphate by isopentenyl diphosphate isomerase.

Isopentenyl diphosphate can also be biologically synthesized by the non-mevalonate pathway. This pathway is prevalent in bacteria and chloroplasts. In the non-mevalonate pathway, pyruvate is condensed with glyceraldehyde 3-phosphate in a series of seven reactions to produce both isopentenyl diphosphate and dimethylallyl diphosphate (Fig. 3) (27). In the first reaction, 1-Deoxy-D-xylulose 5-phosphate is produced by decarboxylating pyruvate and condensed with glyceraldehyde 3- phosphate by 1-Deoxy-D-xylulose 5-phosphate synthase (DXS). 1-Deoxy-D-xylulose 5-phosphate is then reduced and isomerized to 2-C-methylerythritol 4-phosphate (MEP) with the enzyme 2-C-methylerythritol 4-phosphate reductoisomerase (DXR). MEP is then activated with the nucleotide cytosine 5-triphosphate by the 2-C-methyl-D-erythriol 4-phosphate cytidyltransferase (CMS) to 4-diphosphocytidyl-2-C-methylerythritol (CPD-ME) and then phosphorylated by the ATP-utilizing enzyme 4-diphosphocytidyl-2-C-methyl-D-erythritol kinase (CMK) to 4-diphosphocytidyl-2-C-methyl-D-erythritol 2-phosphate (CDP-MEP). CDP-MEP is then converted to 2-C-methyl-D-erythritol 2,4-cyclopyrophosphate (MEcPP) in reaction that forms a cyclodiphosphate intermediate by 2-C-methyl-D-erythritol 2,4-cyclodiphosphate synthase (MCS). The oxidoreductase enzyme 4-hydroxy-3-methylbut-2-en-1-yl diphosphate synthase (HDS) then produces (E)-4-Hydroxy-3-methyl-but-2-enyl pyrophosphate (HMB-PP)

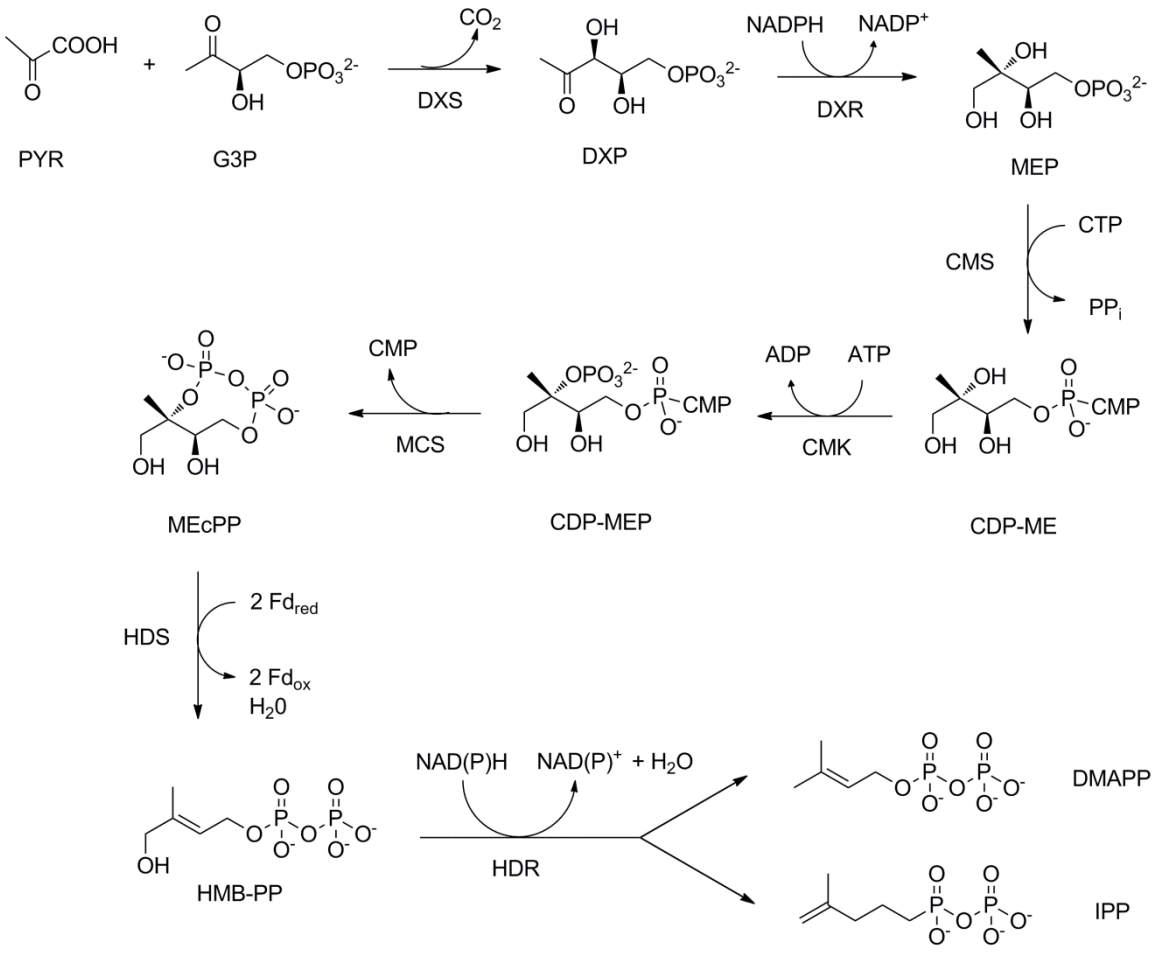

Figure 3. The Non-Mevalonate Pathway. The non-mevalonate pathway is responsible for the production of isopentenyl diphosphate and dimethylallyl disphosphate from pyruvate and glycerol 3-phosphate. This pathway is most commonly used by bacteria and chloroplasts.

from (MEcPP). HMB-PP is then converted to isopentenyl diphosphate or dimethylallyl diphosphate by HMB-PP reductase (HDR).

Multiple lines of experimental evidence strongly suggest that archaea use the mevalonate pathway rather than the non –mevalonate pathway for the production of the isoprenoids used in lipid membrane biosynthesis. The first evidence came from early metabolite radiolabeling experiments performed with [^{14}C] acetate and [^{14}C] mevalonate. Acetate and mevalonate are critical metabolites in the mevalonate pathway (26). These simple but profound experiments showed that radiolabeled carbon from acetate or mevalonate was incorporated into the lipid membrane (28,29). Further examination of the radiolabel pattern in the isoprenoid based lipid membrane also matched the predicted pattern if the metabolites had been processed via the mevalonate pathway (28,29). Subsequent experiments showed that radiolabeled carbon from leucine was also incorporated into the lipid membrane (30). This was suggested to be attributable to either leucine degradation to acetate, HMG-CoA, or another unknown leucine degradation pathway (30). The next indication that the mevalonate pathway was responsible for the production of isoprenoids in archaea came from genome sequencing and annotation. *M. jannaschii* was one of the first genomes ever sequenced (31). Analysis of the sequencing results revealed potential homologs to a few mevalonate pathway enzymes. Additional mevalonate pathway homologs were discovered as more archaea genomes were sequenced in their entirety. Moreover, open reading frames encoding enzymes of the non-mevalonate pathway have yet to be detected in any archaea. The incorporation of mevalonate pathway intermediates, the detection of mevalonate pathway open reading

frames, and the inability to detect any homologs of non-mevalonate pathway enzymes in any archaea suggests that mevalonate metabolism is solely responsible for lipid biosynthesis in archaea.

Functional demonstrations of a few of the classical mevalonate pathway enzymes from various representatives of domain Archaea gave additional support for the existence of an intact mevalonate pathway. The most famous classical mevalonate pathway enzyme, HMG-CoA reductase, has been isolated and enzymatically characterized from *H. volcanii* and *S. solfataricus*. As a domain, archaea possess both the NADPH dependent class-I (32,33) and NADH dependent class-II (34) forms of the enzyme. However, the NADPH dependent class-I HMG-CoA reductase is more prevalent (35, 36). Mevalonate kinase, another classical mevalonate pathway enzyme, has been enzymatically characterized and its structure determined from *M. jannaschii* (37) and in *M. mazei* (38,39). The mevalonate kinase (MK) from *M. mazei* has been reported to be resistant to feedback inhibition from downstream metabolites (38). Bacterial MKs exhibit this same resistance (40,41,42) which stands in contrast to the sensitivity demonstrated by MKs from the eukaryotic domain (43,44). The final enzyme of the classical mevalonate pathway, isopentenyl diphosphate isomerase (IDI), has been isolated (45, 46) and crystallized (47,48). The isopentenyl diphosphate isomerase isolated from archaea was designated a type-II IDI due to low sequence similarity (35). Using newly sequenced genomes, the enzymes described above have been shown to be conserved across the entire Archaeal domain (36). The conservation of these enzymes indicates that an intact pathway for mevalonate metabolism is in operation in the entire domain.

Despite the knowledge that some mevalonate pathway enzymes have been discovered and shown to be conserved across the archaeal domain, a number of classical mevalonate pathway enzymes have remained unidentified and thus uncharacterized. The first committed step of the mevalonate pathway, HMG-CoA synthase, has been annotated in a number of archaeal genomes. The enzyme has been proposed to be conserved across the entire domain (36) but a functional demonstration of the enzyme remains to be documented (35). The terminal reactions of the classical mevalonate pathway, catalyzed by phosphomevalonate kinase (PMK) and mevalonate diphosphate decarboxylase (MDD), have only been demonstrated in *S. solfataricus* (49). However, the grouping and phylogenetic analysis of the open reading frames that encoded the PMK and MDD reveal that *Sulfolobus* likely obtained an entire mevalonate pathway operon by lateral gene transfer (50). This proposal is also supported by the inability to detect homologs to those enzymes in any other archaeal genome (36). Thus, the evidence provided from *S. solfataricus* regarding the terminal reactions of the mevalonate pathway in archaea represents the terminal reactions from *Sulfolobus* only. While this is an important finding, the terminal reactions of the mevalonate pathway in the rest of the archaea remain unclear. Homologs to either eukaryotic or bacteria forms of the enzymes PMK or MDD are absent in the vast majority of sequenced archaeal genomes. There are a few exceptions, as open reading frames from a limited group of archaea present themselves as possible classical mevalonate pathway enzymes. For instance, potential homologs to MDD have been noted in the order Haloarchaea and Thermoplasmatales (36). However, the classical mevalonate pathway

enzyme PMK has not been detected in any of those genomes providing even more uncertainty to the identification of those putative MDDs and of these reactions.

Further, an enzyme from *M. jannaschii* was discovered that suggested that archaea may use an alternate route in mevalonate metabolism. This enzyme, isopentenyl monophosphate kinase (IPK), uses isopentenyl monophosphate and ATP as substrates and facilitates the transfer of the gamma phosphate from ATP to isopentenyl monophosphate (51). The result of this enzymatic reaction is the classical mevalonate pathway product isopentenyl diphosphate. The slight difference in substrates yet the identity of the product as a classical mevalonate pathway intermediate prompted the hypothesis that this enzyme may represent a portion of an alternate route in mevalonate metabolism (Fig. 2) (51). The location of the open reading frame that encodes IPK provided additional support for this hypothesis. IPK is encoded by an open reading frame that is immediately downstream of the classical mevalonate pathway enzyme, mevalonate kinase. The close proximity of the two enzymes suggested they may be part of an operon and perhaps involved in the same pathway. The potential for a mevalonate operon along with the function of IPK provided a reasonable explanation for mevalonate metabolism. To further support this hypothesis, homologs to IPK have been detected in virtually every archaeal genome (36) and functional demonstrations and structures of the enzyme have been provided (51,52,53,54). The conservation and functional demonstrations across the archaeal domain suggests that this enzyme is not unique to the hyperthermophile, *M. jannaschii*, but represents an alternate and conserved route of mevalonate metabolism. However, in order for IPK to be part of an alternate version of the mevalonate pathway in archaea, an enzyme or series of enzymes

would have to exist that could bridge the gap between mevalonate kinase and isopentenyl monophosphate kinase. The shortest route would be a novel phosphomevalonte decarboxylase which has never been demonstrated to exist anywhere in nature.

Despite the accumulated evidence that archaea use the mevalonate pathway, enzymes of the mevalonate pathway remain poorly characterized and parts of the mevalonate pathway remain unclear. This can be attributed to a lack of experimental tools and the difficulty in obtaining protein suitable for enzymatic studies. While there are several archaeal species currently being studied each with their own advantages and disadvantages as model systems, the tools for a robust investigation lag behind other model species from the other two domains. This lack of tools is usually attributed to the extreme environments that archaea typically inhabit. For instance, the challenges in developing genetic tools for *M. jannaschii*, an archaeon that grows under high temperature and pressure, remain formidable. The same challenges exist for archaea that require anoxic environmental conditions which comprise a large portion of the currently known archaeal species. These environmental considerations also make culturing these organisms difficult. For many archaea, specialized and dedicated facilities are required. The difficulty in culturing creates a scarcity of native protein which could be isolated for enzymatic studies. Genomic DNA for sub-cloning into traditional expression systems is also generally limited. Even when genomic DNA is available, the expression of archaeal proteins in traditional expression systems is not always productive. As archaea adapted to extreme environments, their proteins have adapted to operate in these conditions. Open reading frames from these organisms expressed using traditional systems commonly results in the expression of insoluble protein.

Traditional expression systems cannot provide the extreme conditions that archaeal proteins have adapted.

Recently, technology was developed that allows for the overexpression of archaeal proteins in the halophilic archaeon, *H. volcanii* (55). Such an approach appeared to offer a productive way to isolate active forms of mevalonate pathway enzymes, and to ultimately explore cryptic reactions in the MVA pathway of Archaea. This expression system includes a plasmid and host strains suitable for overexpression of target protein (56). The plasmid, pTA963, encodes both an *E. coli* and *H. volcanii* origin of replication allowing it to function as a shuttle vector between *E. coli* and *H. volcanii* (55). pTA963 also encodes an ampicillin resistance gene (55). This allows the plasmid to be amplified to suitable quantities, manipulated using standard recombinant tools, and selected for in *E coli* for transformation into *H. volcanii*. The plasmid also encodes a recombinant sub-cloning site directly downstream of a 6x-His tag and tryptophan inducible promoter (55). This allows for the inducible expression of N-terminal 6-His tagged target protein that can be isolated by Ni-column chromatography. Rescue copies of *pyrE2* (uracil) and *hdrB* (thymidine) on pTA963 allow for the selection of *H. volcanii* strain H1209 (ΔpyrE2 ΔhdrB Δmrr Nph-pitA) transformants (57). *H. volcanii* strain H1209 cannot synthesize uracil or thymidine and transformants can be selected for on media deficient in either or both (56). *H. volcanii* is also easily cultured and can be readily grown in either liquid or solid media with a doubling time of ~2 hours. The ability to cultivate or potentially express functional archaeal enzymes suggested that this approach could provide a realistic opportunity to explore enzymes of the mevalonate pathway in Archaea.

To identify the missing mevalonate pathway enzymes in Archaea, a candidate screen was performed to identify potential open reading frames from the *H. volcanii* genome for expression and characterization. The candidate screen was performed with BlastP and PSI-Blast using bacterial and eukaryotic versions of the classical mevalonate pathway enzymes, HMG-CoA synthase, phosphomevalonate kinase, and mevalonate diphosphate decarboxylase as queries, against the sequenced *Haloferax volcanii* genome as a database. Potential hits were sub-cloned into recently developed plasmids and transformed into host strains suitable for overexpression of protein in a *Haloferax* host. Recovery of active enzyme has provided the first demonstration of an archaeal HMG-CoA synthase and a novel phosphomevalonate decarboxylase. These enzymes along with previously documented archaeal mevalonate pathway enzymes provide, for the first time, a direct route for mevalonate metabolism in *H. volcanii*. The results of these experiments also provide evidence for the operation of an alternate mevalonate pathway in the third domain of life.

CHAPTER 2

MATERIALS AND METHODS

Materials

Acetyl-CoA and acetoacetyl-CoA were chemically synthesized by combining free Coenzyme A with acetic anhydride and diketene, respectively (58). (*R,S*)-mevalonate 5-phosphate and (*R,S*)-mevalonate diphosphate were previously synthesized according to Wang & Miziorko (59) and Reardon & Abeles (60). (*R*)-Mevalonate 5-P, (*R*)-fluoromevalonate monophosphate and (*R*)-fluoromevalonate diphosphate were synthesized enzymatically according to the methods described by Voynova (61). Isopentenyl monophosphate was synthesized as described by Chen and Poulter (53). Hymeglusin was supplied by M.D. Greenspan (Merck Research Laboratories). *E.coli* JM109 and BL21(DE3) cells were purchased from Promega. *H. volcanii* H1209 (Δ*pyrE*2 Δ*hdr*B Δ*mrr Nph-pit*A) and *E.coli* XL1-Blue cells containing the plasmid pTA963 were generously provided by Dr. Thorsten Allers and Dr. Julie Maupin-Furlow. Mevalonate diphosphate decarboxylase from *Streptococcus epidermidis* and 3-hydroxy-3-methylglutaryl CoA synthase from *Enterococcus faecalis* was provided by Dr. Brian Geisbrecht. Isopentenyl monophosphate kinase from *H. volcanii* was provided by Rana Zalmai and Dr. Andrew Skaff. Oligonucleotides were purchased from Integrated DNA technologies. All other chemical or biological products were purchased from Fisher Scientific, Sigma-Aldrich-Fluka or Promega Corporation.

HMG-CoA Synthase from *Haloferax volcanii*

Cloning, Overexpression, and Purification of HMG-CoA

Synthase from *H. volcanii*

An *H. volcanii* open reading frame (HVO_2419) annotated as a putative *Hv*HMGCS that successfully aligned (BlastP) with bacterial and animal HMG-CoA synthases was amplified from genomic *H. volcanii* H1209 DNA by polymerase chain reaction adding 5' EcoRI and 3' BamHI restriction sites. The PCR product and pTA963 were digested using EcoRI and BamHI endonucleases and ligated using T4 DNA ligase. This vector directs tryptophan inducible expression of an N-terminally 6-His-tagged *Hv*HMGCS protein. pTA963-*Hv*HMGCS was transformed into *E. coli* JM109 cells and incubated in LB-amp (50 µg/mL). The plasmid was isolated by a Promega Miniprep kit and then DNA sequenced at the UMKC DNA Core Facility. pTA963-*Hv*HMGCS was then transformed into *H. volcanii* H1209 cells and positive transformants were selected for by growth on Hv-Ca plates (55). Hv-Ca plates are deficient in uracil and thymidine and rescue copies of pyrE2 (uracil) and hdrB (thymidine) on pTA963 allow for the selection of transformants of *H. volcanii* H1209 (ΔpyrE2 ΔhdrB Δmrr Nph-pitA) (55). 5mL of Hv-YPC media was inoculated with individual colonies and grown for 2 days at 45^{o}C with shaking at 200 rpm, then glycerol added to a final concentration of 20% and stored at -80^{o}C. 5mL of Hv-YPC media in sterile culture tubes was then inoculated with frozen transformed cells and incubated at 45^{o}C at 200 rpm for 2 days and then transferred to 50mL of Hv-YPC media and incubated at 45^{o}C and 200 rpm overnight. For expression of the target protein, 50mL of cell culture was transferred to three, 2.5L baffled flasks with 1L of Hv-YPC media and cells were incubated with 1.3mM tryptophan at 42^{o}C with shaking at 200 rpm. After 16 hours, additional tryptophan was added to a final concentration of 3mM and incubation continued for 2 hours at 42^{o}C at 200

rpm. Cells were then pelleted at 6,000 x g for 10 minutes at 4^{o}C; the supernatant was removed, and cells were resuspended in 100mM Tris-Cl (pH 8), 2M KCl, 1mM DTT. Cells were homogenized using a microfluidizer and the lysate centrifuged at 11,000 x g at 4^{o}C. His-tagged protein was isolated by gravity Ni-column chromatography using a gradient maker (40mL total) from 20mM to 200mM imidazole. Fractions free from contaminants as judged by SDS-page gel electrophoresis were pooled and imidazole was removed by passing the eluant over a Sephadex G-50 size-exclusion column. Fractions with activity were pooled and concentrated using a 20mL, 10kD Millipore concentrator at 7,500 x g for 15 minutes. Protein yield was 1.5 mgs per liter of media.

*Hv*HMGCS Molecular Weight Estimate Determination

The molecular mass of *H. volcanii* HMG-CoA synthase (*Hv*HMGCS) was determined by MALDI-TOF MS. *Hv*HMGCS was desalted using reversed phase matrix (C18 ZipTip, Milipore) and eluted directly onto the MALDI plate using 50% acetonitrile containing 10mg/mL sinapinic acid matrix (3,5-dimethoxy-4-hydroxy cinnamic acid). MALDI-TOF (Perseptive Biosystems Voyager DE Pro) was performed in positive, linear mode, acquiring 100 scans per spectrum, with the estimate of 51975 Da representing the average of 5 spectra.

Enzyme Assay, Characterization of Salt, pH, Temperature Dependence of *Hv*HMGCS

Spectrophometric activity assays were performed on a Perkin Elmer λ19 equipped with a water bath for temperature control or a Perkin Elmer λ35 equipped with Peltier temperature controller. Dependence of enzyme activity on salt concentration was

measured by monitoring the disappearance of acetoacetyl-CoA at A_{300} (ε = 3.6 $mM^{-1}cm^{-1}$) in 100mM Tris-Cl, pH 8, at 30°C, containing acetyl-CoA (250µM), acetoacetyl-CoA (10µM), and 0, 1, 2, 3, or 4M NaCl or KCl. Observation of protein concentration dependent catalytic activity confirmed that the open reading frame does, in fact, encode *Hv*HMGCS. The pH dependency of *Hv*HMGCS enzyme activity was measured by the same assay by increasing pH in 0.5 increments from 7.5-10 using 100mM Tris-Cl (7.5-9), or 100mM CHES-K (9.5-10) in 4M KCl at 30°C. Extinction coefficients (300 nm) appropriate for each pH value were utilized in calculating enzyme rates. Temperature dependence was determined by increasing assay temperature by 5°C increments from 25-60°C in 100mM Tris-Cl, pH 8, 4M KCl; activity was monitored by the same 300 nm assay.

Kinetic Characterization of HMG-CoA Synthase from *H. volcanii*

To determine the V_{max} and the K_m and for acetyl-CoA, *Hv*HMGCS was incubated in 100mM Tris-Cl, pH 8, 4M KCl at 30°C with acetoacetyl-CoA (10µM). The reaction was started by the addition of various concentrations (6.25-400µM) of acetyl-CoA and activity was determined by monitoring the disappearance of acetoacetyl-CoA at A_{300}. V_{max} and K_m for acetoacetyl-CoA were determined at 30°C by incubating *Hv*HMGCS in 100mM Tris-Cl, pH 8, 4M KCl and 250µM acetyl-CoA using the HMG-CoA synthase DTNB assay, which estimates reaction velocities equivalent to those observed using the acetoacetyl-CoA based A_{300} assay (62). The reaction, performed at 250µM DTNB, measures the rate of CoA-SH production and is started by the addition of various concentrations (0.25-100µM) of acetoacetyl-CoA. The data obtained were analyzed using non-linear regression analysis with Graph Pad 5.0.

Similarly, purification and kinetic characterization of *E. faecalis* HMGCS were performed using methods previously documented by Skaff et al. (63).

Inhibition of Purified *Hv*HMGCS by Hymeglusin

Enzyme activity was measured at 412 nm by the HMG-CoA synthase DTNB assay (62). Purified *Hv*HMGCS (49nM) was incubated with hymeglusin (100-400nM) in 100mM Tris-Cl pH 8, 4M KCl at 18^{o}C. This lower temperature diminishes the reaction rate and allows inhibition to be studied at inhibitor concentrations approximating those appropriate for Michaelis-Menten kinetic analysis. Saturating levels of acetyl-CoA (250µM) were added at specified time points to acetylate any free enzyme and block hymeglusin from forming additional inactivated enzyme. Acetoacetyl-CoA (10µM) was added to start the reaction, which was measured at 412 nm using 250µM DTNB. The data were fitted to semilog plots of residual activity versus time using a linear model. Nonlinear regression analysis (Graph Pad Prism 5.0) was used to determine K_i and k_{inact}.

Growth Inhibition of *H. volcanii* H1209 Culture by Hymeglusin

Three samples (10mL) of Hv-YPC supplemented with thymidine (60 µg/mL) were inoculated with an overnight culture of *H. volcanii* H1209 to an A_{600} of 0.050 and grown in the presence or absence of hymeglusin (25µM) for 4 hours at 45^{o}C and 200 rpm. Cells were pelleted at 6000 x g for 10 minutes and resuspended in fresh Hv-YPC media (10mL) supplemented with thymidine (60 µg/mL). The samples (1.5mL) were plated in 24-well plates and incubated at 45^{o}C and 200 rpm in the presence or absence hymeglusin (25µM) with A_{600} measured at the indicated times using a Biotek H1 synergy plate reader. Data represent an average of three replicates.

Phosphomevalonate Decarboxylase from *Haloferax volcanii*

Identification, Cloning, and Overexpression of *Hv*PMD

Protein sequences encoding bacterial and eukaryotic mevalonate diphosphate decarboxylases were obtained from NCBI and used as queries and aligned against the *H. volcanii* genome as a database using BlastP and PSI-Blast. The BlastP alignment was performed with general parameters of 10 and 3, respectively for expect threshold and word size with Blosum62 as the scoring matrix and gap cost existence 11 and extension 1. PSI-Blast was performed using the same parameters above except with the addition of a PSI-Blast threshold of 0.005 and performed to convergence. An open reading frame (HVO_1412) that successfully aligned to both was PCR amplified from *H. volcanii* H1209 genomic DNA using Pfu polymerase with the addition of 5' EcoRI and 3' BamHI restriction cut sites. The PCR product and pTA963 were restriction digested using EcoRI and BamHI and ligated using T4 DNA ligase. Ligations was transformed into *E. coli* JM109 cells and incubated in LB-amp (50 µg/mL). The plasmid was isolated by a Promega Miniprep kit and then DNA sequenced at the UMKC DNA Core Facility. Plasmid was then transformed into *H. volcanii* H1209 cells and stored in 20% glycerol at -80^{o}C as previously described (64). Frozen cells were then inoculated into five milliliters of Hv-YPC and grown for two days at 45^{o}C at 200 rpm, then added to fifty milliliters of Hv-YPC and grown at 45^{o}C at 200 rpm. For protein overexpression, fifty milliliters of cell culture was transferred to two, 2.5 liter baffled flasks containing 1L of Hv-YPC medium and grown for 16 hours at 42^{o}C at 200 rpm in the presence of 1.3mM tryptophan and then for 1 hour with 3mM tryptophan.

For *H. volcanii* H1209 cells transformed with pTA963-*Hv*PMD, cells were pelleted at 6000 x g at 4^{O}C, the supernatant removed, and then resuspended in 100mM Tris-Cl (pH 7.5), 2M KCl, 20mM imidazole, 1mM DTT, 1mM PMSF. The cell suspension was then homogenized by microfluidization and the cell lysate was centrifuged at 11,000 x g at 4^{O}C for 30 minutes. *Hv*PMD His-tagged protein was isolated from the cell lysate by gravity Ni-column chromatography using a step-wise gradient of 40mM and 200mM imidazole in 100mM Tris-Cl (pH 7.5), 2M KCl, 1mM DTT. Imidizole was removed by passing the eluate over a Sephadex G-25 column. Fractions exhibiting enzymatic activity were pooled and concentrated using a 20mL, 10 kDa cutoff Millipore concentrator at 5,000 x g for 15 minutes at 4^{O}C. The yield was 2 mgs of purified protein per liter of culture.

*Hv*PMD Molecular Weight Estimate Determination

The molecular mass of *Hv*PMD was determined by matrix assisted laser desorption ionization-time of flight (MALDI-TOF) mass spectrometery using a Perseptive Biosystems Voyager DE Pro operating in a positive, linear mode. *Hv*PMD was desalted (C18 Zip Tip; Millipore) and eluted onto the MALDI plate with 50% acetonitrile containing 10mg/mL sinapinic acid (3,5 dimethoxy-4-hydroxycinnaminic acid) matrix for these analyses.

Enzyme Assay and Characterization of Salt and pH Dependence

Enzymatic activity in this study was monitored by measuring the appearance of ADP using a pyruvate kinase/ lactate dehydrogenase coupled assay with a Perkin Elmer λ35 with a Peltier temperature controller or an Agilent Systems Cary 60 UV-Vis spectrophotometer with a water bath for temperature control. The dependence of *Hv*PMD activity on salt concentration was assayed in 50mM Hepes-KOH (pH 7.5), 10mM $MgCl_2$, with 40 units of

both pyruvate kinase and lactate dehydrogenase from rabbit muscle in increasing concentrations of KCl from 0-4M in the presence 2mM (*R,S*) mevalonate 5-P and 2mM ATP at 30^{o}C. The dependence of pH on *Hv*PMD enzyme activity was performed using the same assay by in increasing 0.5 pH increments from 6.5-8.5.

*Hv*PMD Kinetic Characterization

The V_{max} and K_m for *Hv*PMD were determined for (*R,S*)-mevalonate 5-P and (*R*)-mevalonate 5-P by incubating *Hv*PMD in 50mM Hepes-KOH (pH 7.5), 10mM $MgCl_2$, 400µM PEP, 200µM NADH, 2mM ATP, and 4 units of both pyruvate kinase and lactate dehydrogenase at 30^{o}C. The reaction was started by the addition of increasing amounts of (*R,*S)-mevalonate 5-P or (*R*)-mevalonate 5-P from 12.5-3200µM; reaction progress was monitored at A_{340}. The V_{max} and K_m for ATP was determined by incubating *Hv*PMD in 50mM Hepes-KOH (pH 7.5), 10mM $MgCl_2$, 400µM PEP, 200µM NADH, 4 units of both pyruvate kinase and lactate with increasing amounts of ATP from 20-4000µM at 30^{o}C. The reaction was started with the addition of 2mM (*R,S*) mevalonate 5-P. Data were analyzed using Graph Pad 5.0.

Enzymatic and Mass Determination of the *Hv*PMD Reaction Product

20µg of *Hv*PMD was incubated in a one mL cuvette containing 50mM Hepes-K (pH 7.5), 10mM $MgCl_2$, 200 nmoles of NADH, 400 nmoles of PEP, 2 µmoles of ATP, and 4 units of pyruvate kinase and lactate dehyhdrogenase at 30^{o}C. The reaction was started with the addition of 100, 150, or 200 nmoles of (*R,S*)-mevalonate 5-P and the disappearance of NADH was monitored at A_{340}. The amount of (*R,S*)-mevalonate 5-P converted to product was determined by the reaction end-point. To test for the presence of mevalonate 5-

diphosphate after the initial reaction had gone to completion, mevalonate diphosphate decarboxylase from *S. epidermidis* (*Se*MDD) was added to the reaction mixture. The reaction was allowed to go to completion and the amount the product formed was determined by the reaction end-point. To test whether the reaction had instead produced isopentenyl-phosphate, isopentenyl-phosphate kinase from *H. volcanii* (*Hv*IPK) was added to the reaction mixture and the disappearance of NADH was again monitored at A_{340}. The reaction was allowed to go to completion and the amount the product converted was determined by the end-point. Reaction stoichiometries were calculated on the basis of the nmoles of substrate converted to nmoles of product, based on these assay end-points. To identify the product of *Hv*PMD by mass spectrometry, four milliliters of 50mM Tris-Cl (pH 7.5), 10mM $MgCl_2$, 625µM (*R,S*) mevalonate 5-P, and 2mM ATP were incubated at 40^{o}C for 30 minutes in the presence or absence of 25µg of *Hv*PMD. Twelve milliliters of ice cold of USP 190 proof ethanol was then added to precipitate nucleotides and the samples were centrifuged at 16,000 x g for 15 minutes at 4^{o}C. The supernatant was separated from precipitate and ethanol removed by rotary evaporation. The samples were mixed with 20mM triethylammonium-bicarbonate (TEA-HCO_3), (pH 8.5) buffer and passed over a Sephadex A-25 (2 ml resin in 5mm diameter) column. The column was washed with 5 column volumes of 20mM TEA-HCO_3 (pH 8.5) and compounds eluted using an increasing step-wise gradient of 100mM TEA-HCO_3 from100mM to 500mM. The TEA-HCO_3 buffer was then removed by rotary evaporation. The reaction substrate and product were then detected and verified by electrospray ionization mass spectrometry (nanospray, ESI-MS) using a Thermo Finnigan LTQ linear ion trap MS system. Samples were diluted in 80%

water:20% acetonitrile to approximately 100 pmole per L for direct infusion at 1 to 3 µL per minute after equilibration by syringe pump. The mass analyzer was operated in negative mode, acquiring centered (centroid) or profile data. At least 20 seconds of scans (multiple spectra) were averaged to generate figures, with apparent unit resolution. Phosphorylated ions (or phosphate ions) were detected in single charge state under these conditions, with monoisotopic masses resolved within 0.1 Da (~ 500 ppm).

IC_{50} Determination for (*R*)-fluoromevalonate 5-P and (*R*)-fluoromevalonate 5-PP Against *Hv*PMD

(*R*)-fluoromevalonate 5-P or (*R*)-fluoromevalonate 5-PP were serially diluted 2-fold from 200µM-0.39µM in 50mM Hepes-K (pH 7.5), 10mM $MgCl_2$ in a 96-well plate. 50mM Hepes-K (pH 7.5), 10mM $MgCl_2$, 400µM PEP, 200µM NADH, 2mM ATP, 10µg/mL of *Hv*PMD, and 4 units of both pyruvate kinase and lactate dehydrogenase were added as a final concentration to each well of the 96-well plate. The reaction was started with the addition (*R,S*)-mevalonate 5-phosphate as a final concentration of 150µM. Enzymatic activity was monitored at A_{340} for 5 minutes at 30^{o}C in a Molecular Devices SpectraMax 250, 96-well plate reader. Data were analyzed by Graph Pad 5.0.

CHAPTER 3

EXPRESSION, CHARACTERIZATION, AND ESSENTIALITY OF 3-HYDROXY-3-METHYLGLUTARYL SYNTHASE FROM *H. VOLCANII*

Introduction

3-Hydroxy-3-methylglutaryl CoA synthase (HMGCS) catalyzes the first committed step of the mevalonate pathway. This enzyme is responsible for the physiologically irreversible condensation of acetyl-CoA and acetoacetyl-CoA to 3-hydroxy-3-methylglutaryl CoA (26). The importance of HMG-CoA synthase for the mevalonate pathway and the production of isoprenoids is made evident by the proven conservation and essentiality in at least two of the three domains of life. Functional demonstrations of the enzyme have been provided in both native and recombinant forms from a number of representatives from domain Eukarya notably *S. cerevisiae* (65) and *H. sapiens* (66). Recombinant HMG-CoA synthase has also been isolated and characterized from *S. aureus* (67) and *E. faecalis* (63) of the bacterial domain. The essentiality of the enzyme has been demonstrated by knockout experiments in *S. pneumonia* (68) and yeast (69).

Archaea represent an evolutionarily distinct domain of microorganisms and the third domain of life (2). Unlike both the eukaryotic and bacterial domains, they contain an abundance of extremophiles that flourish in conditions of high temperature, acidity, or salinity (70). Archaea do not possess cellular organelles like bacteria yet exhibit eukaryotic traits related to DNA replication, transcription, and protein translation (23). The defining

characteristic of Archaea is their unique lipid membranes. Archaea are characterized by cell membrane lipids that contain, as a major component, polyisoprenoids in ether linkages to glycerol rather than the ester linked fatty acids that characterize membranes of other organisms (21). Metabolite labeling experiments have suggested that archaeal polyisoprenoids derive from isopentenyl 5-diphosphate produced by enzymes of the mevalonate (MVA) pathway (25). Despite the knowledge gained from radiolabeling experiments and annotations to recently sequenced archaeal genomes, there is some uncertainty regarding the enzymes responsible for the mevalonate pathway in Archaea. However, the discovery of an isopentenyl monophosphate kinase suggests that Archaea may use an alternate route in the terminal reactions of the mevalonate pathway although functional demonstration of an archaeal HMG-CoA synthase has not been previously provided.

Characterization of mevalonate pathway enzymes from Archaea has been hindered by the fact that many are extremophiles. The extreme nature of these organisms makes their routine cultivation difficult and thus limits sufficient quantities of native protein for study. The proteins of these extremophiles have also adapted to operation in extreme conditions making expression in mesophilic hosts problematic. Despite the advantage halophilic archaea have in being easily cultured, their enzymes routinely function optimally in high salt levels (>2.5 M). When the open reading frames for such proteins are expressed in bacteria such as *E. coli*, the target protein is typically recovered in insoluble form (55). Denaturation and renaturation processes are commonly attempted with the uncertain goal of recovering functional enzyme from the inactive protein precipitate. Such a process has

met with some success in the case of *E. coli* expression of *Haloferax volcanii* HMG-CoA reductase (33), but widespread success of this approach for production of active enzymes critical to halophilic metabolism remains to be documented.

Recently, technology has been developed and reported for expression of halophilic target proteins in *Haloferax volcanii* (55). Such an approach appeared to offer a productive way to isolate active forms of mevalonate pathway enzymes and to ultimately explore cryptic reactions in the MVA pathway. In order to provide an initial test of this hypothesis, expression of an open reading frame proposed to encode HMG-CoA synthase (*Hv*HMGCS), which catalyzes the condensation of acetyl-CoA with acetoacetyl-CoA in the first irreversible reaction in the mevalonate pathway, was attempted.

Results

Sequence Comparisons of a *Haloferax volcanii* HMGCS with Eukaryotic and Prokaryotic HMGCS Enzymes

The *H. volcanii* open reading frame that encodes a putative HMGCS (HVO_2419) corresponds to a 445 residue protein. In comparison, human cytosolic HMGCS is a 522 residue protein and *S. aureus* HMGCS (mvaS) is a 388 residue protein. BLAST comparison of *Hv*HMGCS and human HMGCS indicates only 30% identity, comparable to the 31% identity indicated by a BLAST of *Hv*HMGCS versus the *S. aureus* enzyme. Despite these low levels of identity, sequence alignment of the archaeal, animal, and bacterial proteins (Fig. 4) makes apparent that several residues critical to catalytic function from both eukaryotic and bacterial forms of the enzyme are conserved in the putative *Hv*HMGCS. Both eukaryotic and bacterial HMGCSs have been shown to employ a cysteine, histidine, and glutamate triad in

the active site. C120 from the putative *Hv*HMGCS open reading frame aligns with the conserved cysteine that contributes the active site thiol (71) involved in forming the acetyl-S-enzyme and CoA-HMG-S-enzyme reaction intermediates (72). H224 from *Hv*HMGCS aligns with the conserved and catalytically important histidine found in both the bacterial and eukaryotic enzyme. This histidine contains the imidazole moiety shown to be important in binding of substrate acetoacetyl CoA (73). This binding contribution is explained by its interaction with both of the oxygen substituents on C1 and C3 of the substrate's acyl group (74). While these *Hv*HMGCS residues are undoubtedly functionally important, there are homologous cysteine and histidine residues in other members of the family of initial condensing enzymes (e.g. β-ketothiolase, as well as the β-ketoacyl synthase of fatty acid biosynthesis). Any ambiguity concerning the functional assignment is, however, removed by the observation of E83 (Fig. 4), which is homologous to the animal HMGCS residue E95, shown to be the catalytic base critical to the condensation reaction (26). For other members of the initial condensing enzyme family, this catalytic base does not exist and is not required. The observation that E83 aligned with conserved and the catalytically important glutamate from both bacteria and eukaryotes suggested that the HMGCS annotation was correct and stimulated the attempt at the expression, isolation, and characterization of HMGCS from this halophile.

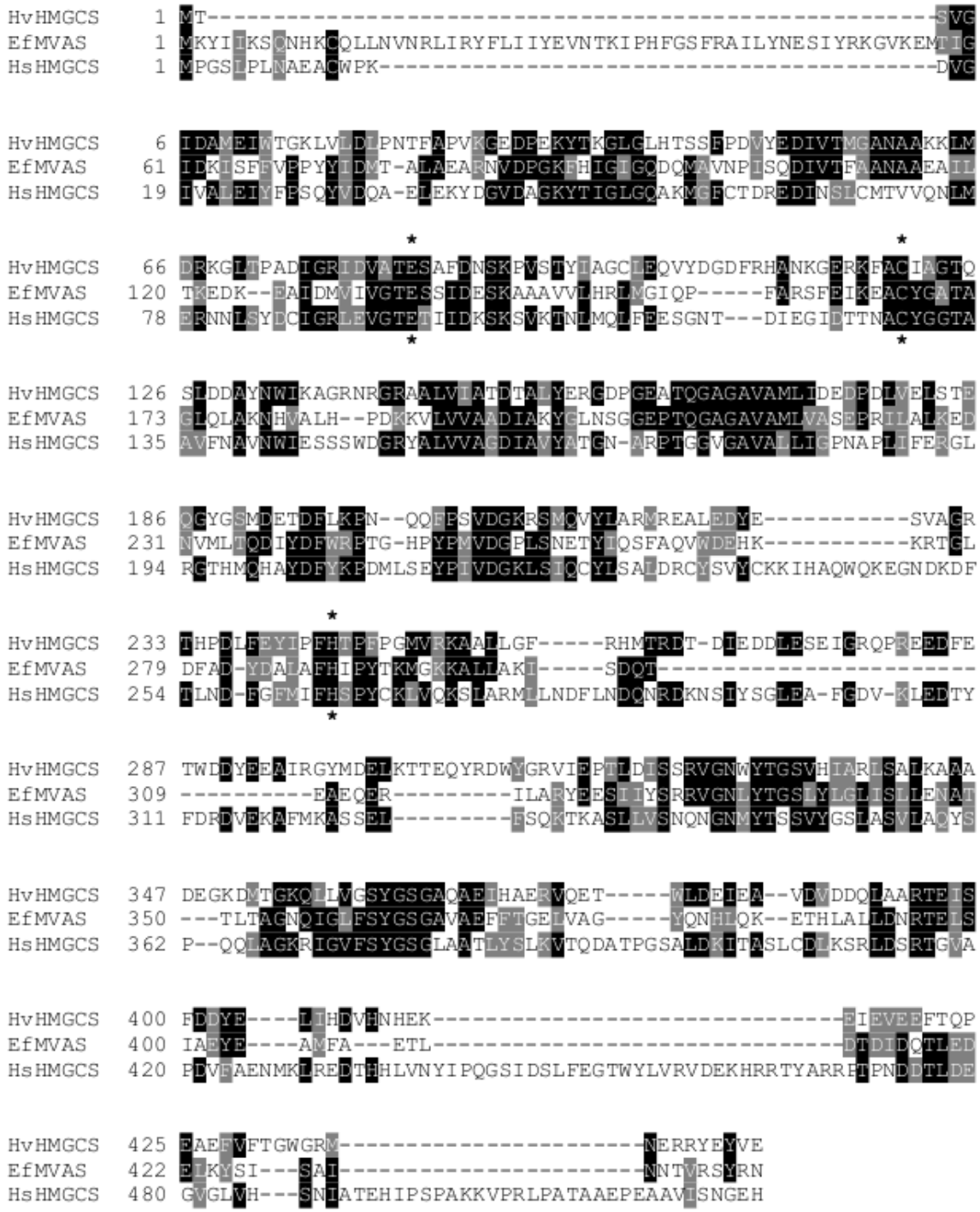

Figure 4. Multiple sequence alignment of HMG-CoA synthase.

Figure 4. Continued. The sequence of HMG-CoA synthase from *H. volcanii* (*Hv*HMGCS) was aligned with a previously characterized HMG-CoA synthase from *E. faecalis* (*Ef*mvaS) and *H. sapiens* (*Hs*HMGCS)**.** Conserved residues are in black and similar residues are in gray. Catalytically important residues are indicated with an asterisk. The alignment was performed by T-Coffee and visualized by Boxshade.

Haloferax volcanii Expression of *Hv*HMGCS

The previously sequenced *Haloferax volcanii* genome deposited to NCBI contained an annotation for an HMG-CoA synthase (75). The multiple sequence alignment of this open reading frame to known bacterial and eukaryotic versions of HMG-CoA synthase showed conservation in known active site residues (Fig. 4) and thus prompted interest in sub-cloning and overexpression in *E. coli*. Initial attempts to express in *E. coli* the open reading frame annotated as *Hv*HMGCS met, not surprisingly, with limited success. The expressed protein target was recovered as a largely insoluble, inactive enzyme. Little HMGCS activity was measured in the supernatant fraction recovered from the lysate of induced bacteria. Host strains and vectors designed for the overexpression of halophilic proteins in an *H. volcanii* host (55) seemed a promising alternative so an expression plasmid encoding the putative *Hv*HMGCS was prepared. The protein was expressed and isolated by Ni-column chromatography to apparent homogeneity as indicated by SDS-page (Fig. 5). A modest level of His-tagged target protein was recovered (1.5 mgs from one liter culture), mainly in the soluble fraction of cell lysates. The protein exhibits substantial HMGCS activity; specific activity of purified enzyme is certainly comparable to values reported for other HMGCS enzymes. The protein's mobility on SDS-PAGE suggests a subunit molecular mass of ~65 kDa, a value much higher than the calculated mass of the expressed protein (51990 Da) and the MALDI estimate of 51975 Da. Anomalies in SDS-PAGE mobility of halophilic proteins have previously been documented (76) and are attributed to their typically high content of acidic residues. In accord with this prediction, *Hv*HMGCS is characterized by a high acidic residue

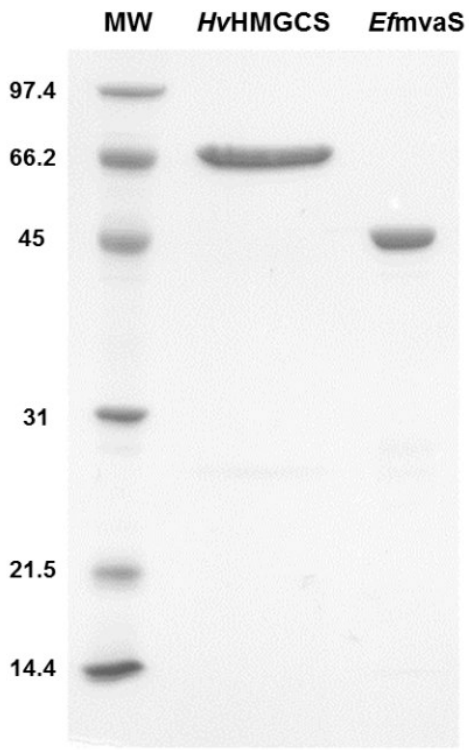

Figure 5. SDS-PAGE Gel of Purified *Hv*HMGCS. *Hv*HMGCS was purified by gradient Ni-column chromatography. Lanes: MW, molecular weight standards (Thermo Scientific PAGE ruler; PI-26616); *Hv*HMGCS, 2 µg of affinity purified *Hv*HMGCS (molecular mass calculated on the basis of amino acid composition, 52.0 kDa); *Ef*mvaS, 2 µg of affinity purified *E. faecalis* MvaS (molecular mass calculated on the basis of amino acid composition, 42.2 kDa). The values to the left are molecular masses in kilodaltions. *Ef*mvaS was provided by Dr. Brian Geisbrecht.

content (42 Asp; 46 Glu; 19.8% of total residues); the pI calculated for HvHMGCS (pI = 4.5) may explain the SDS-PAGE mobility properties. In comparison with the Haloferax enzyme, human HMGCS contains 37 Asp and 28 Glu residues (12.5% of total; calculated pI = 5.2) while S. aureus HMGCS/mvaS contains 29 Asp and 27 Glu residues (14.5% of total; calculated pI = 5.0).

*Hv*HMGCS Salt, pH, and Temperature Dependence

As expected for a halophilic organism, enzyme activity of *Hv*HMGCS increases upon inclusion of either NaCl or KCl in the assay (Fig. 6). There is some advantage with KCl rather than NaCl at a 4M concentration. KCl stimulates catalytic activity by >12 fold over values measured without supplementation with halide salt. The pH rate profile for *Hv*HMGCS indicates an optimum at pH ~8.5 (Fig. 7, Table 2). This value is comparable to reports for the enzyme from eukaryotic (avian, pH = 9.4) and prokaryotic (E. faecalis, pH = 9.8) sources (77,78) and could reflect either ionization state of key amino acids (e.g. at lower pH) or protein instability and lability of the thioester substrates at alkaline pH. The optimum temperature for catalytic activity (Fig. 8, Table 2) is 45°C, in accord with the temperature used to optimize growth of *H. volcanii* (55). For comparison with prokaryotic HMGCS, the enzyme from *Enterococcus faecalis* (77) has a reported optimum reaction temperature of 37°C. The temperature stability of *Hv*HMGCS over extended time periods has been measured (Table 1) in the presence of an excess of acetyl-CoA. The half-life of the active enzyme is 27 hours at 45°C.

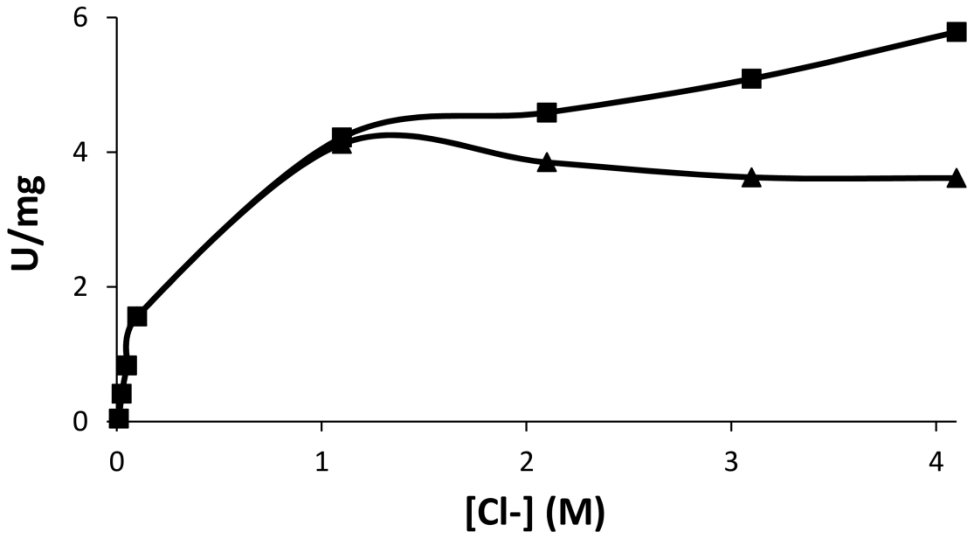

Figure 6. Salt Dependence of *Hv*HMGCS. Activity was measured by monitoring the disappearance of acetoacetyl-CoA at A_{300} at saturating levels for both acetyl-CoA (250µM) and acetoacetyl-CoA (10µM). a) Salt dependent enzyme activity of *Hv*HMGCS was measured in 100mM Tris-Cl, pH 8, at 30^{o}C. Concentrations of KCl (■) or NaCl (▲) ranged from 0 to 4M, as indicated.

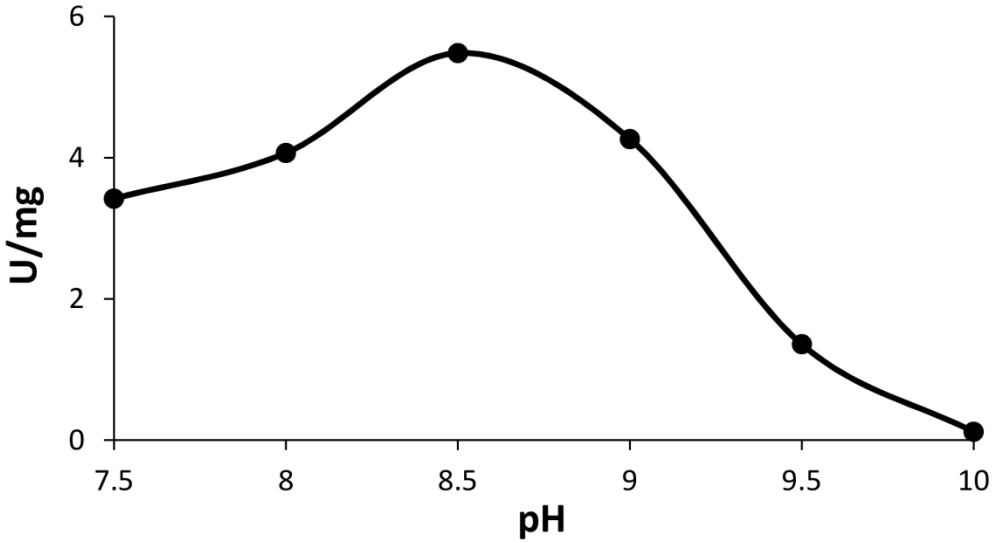

Figure 7. pH Dependence of *Hv*HMGCS. Activity was measured by monitoring the disappearance of acetoacetyl-CoA at A_{300} at saturating levels for both acetyl-CoA (250µM) and acetoacetyl-CoA (10µM). pH dependent enzyme activity (●) was measured over a pH range from 7.5-10 using 100mM Tris-Cl (7.5-9), and 100mM CHES-K (9.5-10) in 4M KCl at 30^{o}C.

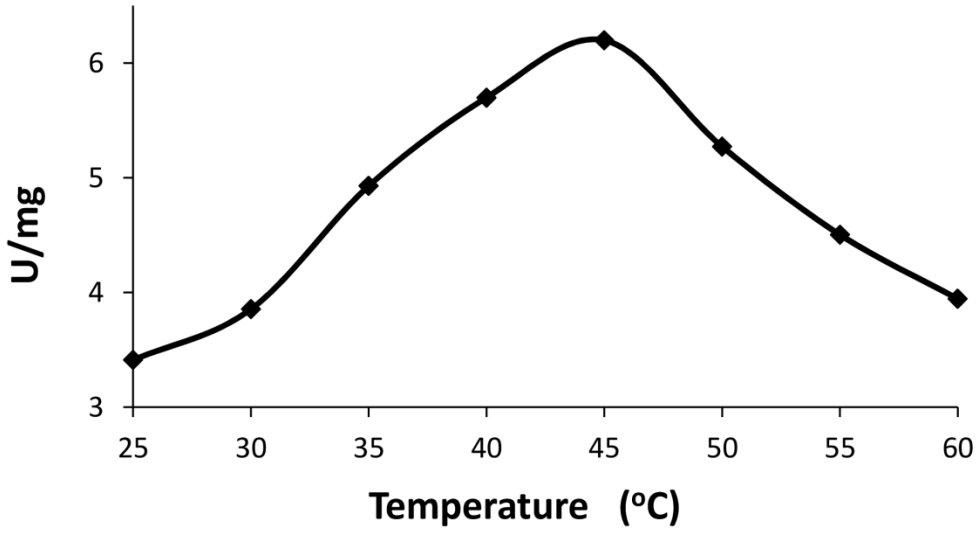

Figure 8. Temperature Dependence of *Hv*HMGCS. Activity was measured by monitoring the disappearance of acetoacetyl-CoA at A_{300} at saturating levels for both acetyl-CoA (250µM) and acetoacetyl-CoA (10µM). Temperature dependent enzyme activity (♦) was measured at 5°C increments over a range of 25-60°C.

Table 1. Activity Profile of *H. volcanii* HMG-CoA synthase

Parameter	Conditions for maximum activity
Optimum [KCl] (M)	4
Optimum pH	8.5
Optimum Temperature (^{o}C)	45
$t_{1/2}$ (h)[a]	27
Organic solvent tolerance	Relative % activity[b]
DMSO 5%	103
10%	79
MeOH 5%	68
10%	41
ACN 5%	89
10%	65

Table 1. Continued

[a]Temperature dependent decay of *Hv*HMGCS activity was monitored in a sample of enzyme with acetyl-CoA (250µM) in 100mM Tris-Cl, pH 8, 2M KCl, 20% glycerol upon incubation at 45^{o}C.

[b]Activity was measured using the 412 nm assay described in the Methods section supplemented with solvents at the levels (%v/v) indicated. Abbreviations used for organic solvents are: DMSO, dimethylsulfoxide; MeOH, methanol; ACN, acetonitrile

Kinetic Properties of *Hv*HMGCS

*Hv*HMGCS exhibits a maximum velocity, V_{max}, of 5.3 U/mg upon a hyperbolic curve fit of observed rates versus variable acetyl-CoA concentrations. The V_{max} = 4.0 U/mg is estimated from a similar fit of rates to variable acetoacetyl-CoA concentrations. These values fall into the range of V_{max} values reported for eukaryotic and prokaryotic HMGCS enzymes (Table 2). The calculated K_m for acetyl-CoA is 50µM, which is lower than most other K_m values in the literature (Table 2). The catalytic efficiency approaches the 10^5 ($s^{-1}M^{-1}$) range similar to values previously reported (Table 2). The dependence of the overall rate of HMG-CoA synthesis upon acetoacetyl-CoA concentration is depicted in Fig. 9 for both *Hv*HMGCS and *Enterococcus faecalis* HMGCS. While data for the latter demonstrate the onset of strong substrate inhibition at [acetoacetyl-CoA] > 2 µM, the data for *Hv*HMGCS are well fit by a hyperbolic saturation curve, providing no indication of comparable substrate inhibition. This kinetic characteristic distinguishes the archaeal enzyme from those eukaryotic (66) and prokaryotic (77) HMGCS enzymes that have been extensively characterized. A K_m for acetoacetyl-CoA = 1.4 µM (Table 2) is estimated for *Hv*HMGCS. A K_m value of 0.5 µM was estimated for the productive binding of acetoacetyl-CoA to the *E. faecalis* enzyme. For non-productive acetoacetyl-CoA binding to the latter enzyme as a substrate inhibitor, the data fit indicates a K_i = 1.9 µM. Thus, for this prokaryotic enzyme, productive and non-productive (inhibitory) binding of second substrate occur at concentration ranges that are not markedly different.

Table 2. Kinetic parameters of HMG-CoA synthases from *H. volcanii,* *E. faecalis,* and *H. sapiens*

Parameter (units)	*H. volcanii* HMGCS	*E. faecalis* HMGCS[b]	*H. sapiens* HMGCS[c]
K_m acetyl-CoA (μM)	50 ± 6	400 ± 60	29 ± 7
K_m acetoacetyl-CoA (μM)	1.4 ± 0.1	0.5 ± 0.1	ND
V_{max} (μmol/min/mg)	5.3 ± 0.2	1.6 ± 0.3	0.7 ± 0.1
k_{cat} (s^{-1})	4.6 ± 0.2	1.1 ± 0.2	0.7
k_{cat} / K_m ($s^{-1}M^{-1}$)	(9.2 ± 1.1) x 10^4	(2.8 ± 0.2) x 10^3	2.3 x 10^4
K_i hymeglusin (nM)	570 ± 120	700 ± 18	53.7
k_{inact} (min^{-1})	17 ± 3	3.5 ± 0.6	1.06

Table 2. Continued

[a] Values are means and standard error of the means.

[b] Data for *E*. *faecalis* HMGCS were previously reported by Skaff et al (63)

[c] Data for *H*. *sapiens* HMGCS were previously reported by Rokosz et al (66). The k_{cat} and $k$cat/K_m values were not explicitly reported but were calculated by using the V_{max} and molecular weight.

[d] ND, not determined.

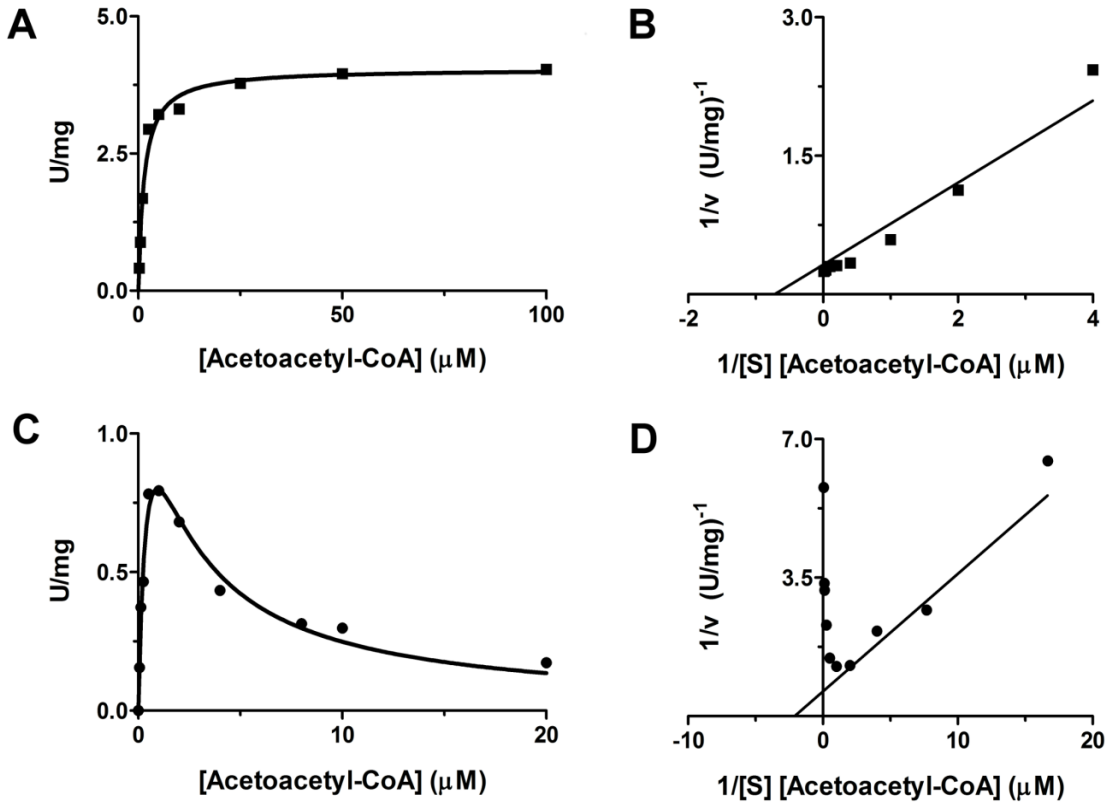

Figure 9. Dependence of *Hv*HMGCS reaction rate on [acetoacetyl-CoA]. Specific activity for both *Hv*HMGCS and *Ef*mvaS for acetoacetyl-CoA was determined by monitoring the production of free CoA in the presence of DTNB at 412 nm in 100mM Tris-Cl, pH 8 at 30^{o}C. a) *Hv*HMGCS (■) assay contained 4M KCl and saturating acetyl-CoA (250μM). b) double reciprocal plot of *Hv*HMGCS (■). c) *Ef*mvaS (●) assay contained saturating acetyl-CoA (500μM). d) double reciprocal plot of *Ef*mvaS (●). Data points represent enzyme activity (U/mg) at the indicated concentrations of acetoacetyl-CoA and were analyzed by Graph Pad 5.0.

Inhibition of *Hv*HMGCS by Hymeglusin

Hymeglusin (Fig. 10) (designated in the literature as 1233A, F244, L-659-699) is a fungal metabolite that exhibits high specificity for inhibition of both the eukaryotic and prokaryotic forms of HMGCS (79). Inhibition occurs upon reaction of its β-lactone functional group with the active site cysteine of HMGCS. This results in a time-dependent loss of activity as the inhibitor forms a thioester linkage to the cysteine (68). In order to test whether C120 of *Hv*HMGCS may react similarly to the active site cysteine of eukaryotic and prokaryotic HMGCS, enzyme was incubated with a range of hymeglusin concentrations and activity monitored over a two minute incubation period (Fig. 11). A time dependent loss in activity is observed; inactivation occurs with first order kinetics, as expected for covalent modification. Computational fits of these data indicate an affinity for hymeglusin (K_i = 570 ± 120nM; Table 1) that is over an order of magnitude weaker than the value (53.7 nM) reported for human HMGCS (66). However, the rate of inactivation (k_{inact} = 17 ± 3 min^{-1}) is an order of magnitude faster than observed for the human enzyme (1.06 min^{-1}). Intrinsic reactivity of C120 may be influenced by thioester access to solvent or by active site residues that interact with this critical amino acid's sulfhydryl to account for these contrasts in the rate of inactivation.

Essentiality of *Hv*HMGCS to *H. volcanii* Cellular Growth

After inactivation experiments demonstrated the sensitivity of *Hv*HMGCS to hymeglusin, it seemed reasonable to determine whether this compound could be useful in

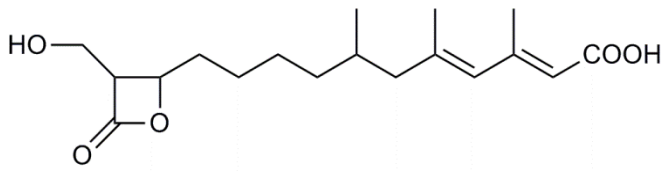

Figure 10. Chemical Structure of Hymeglusin.

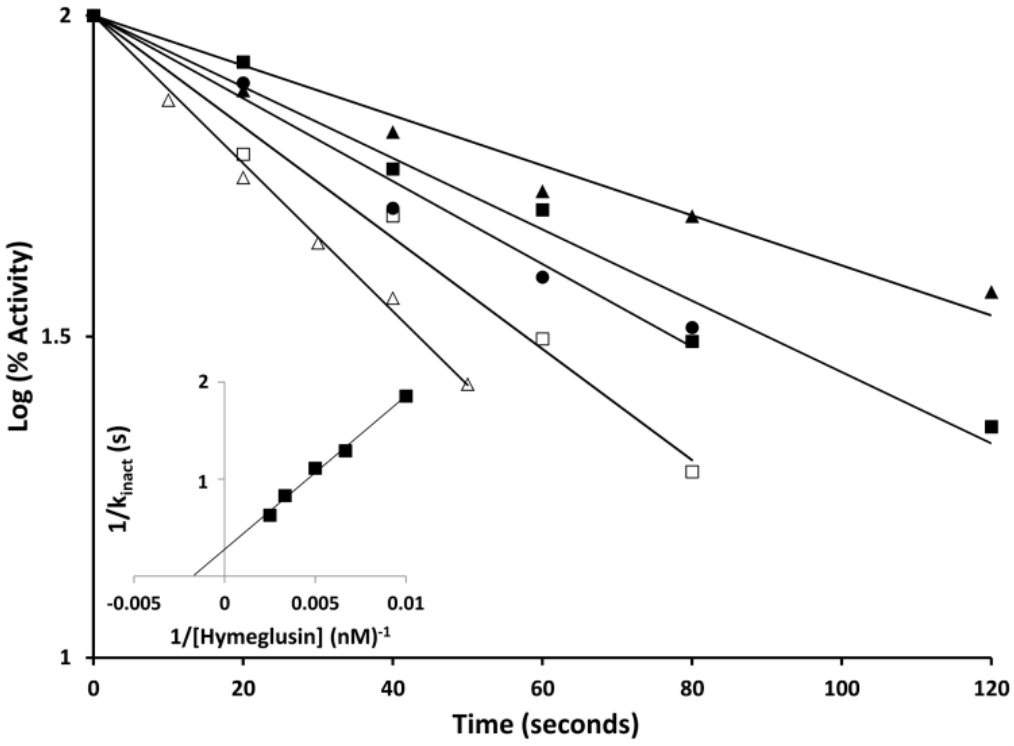

Figure 11. Time Dependent Inactivation of HMG-CoA Synthase from *H. volcanii.*

Figure 11. Continued. Hymeglusin was incubated with purified *Hv*HMGCS protein and the inactivation process was stopped by the addition of acetyl-CoA at the time points indicated. The assay of residual activity was initiated by the addition of acetoacetyl-CoA and the reaction was monitored by absorbance at 412 nm using the DTNB assay described in the Methods section. Concentrations of hymeglusin used were (▲) 100nM, (■) 150nM, (●) 200nM, (□) 300nM, (Δ) 400nM. Progress curves were fit to a linear model using GraphPad Prism 4 with R^2 values greater than 0.97 for all time courses. Inset: replot of the reciprocal of the apparent $k_{observed}$ values (derived from $t_{1/2}$ values of data sets depicted in the main figure) versus the reciprocal of hymeglusin concentration. From this double reciprocal plot, the x- and y-intercepts were used to determine the K_i = 570 ± 120 nM and k_{inact} = 17 ± 3 min^{-1}, respectively.

an *in vivo* test of the importance of *Hv*HMGCS and, by inference, the mevalonate pathway to essential metabolism in *Haloferax volcanii*. In this experiment, *H. volcanii* H1209 cells were grown for 4 hours in the presence or absence of 25µM hymeglusin. This level of hymeglusin was chosen because it represents a concentration in sufficient excess to inactivate *Hv*HMGCS. Cells were separated from medium by centrifugation. At t=0 hours, the untreated cells were resuspended in fresh medium (without hymeglusin) while the cells previously treated with hymeglusin were resuspended in medium that contained either 0 or 25 µM hymeglusin. The growth of cells (incubated at 45°C) in these three samples was monitored (A_{600}) for 36 hours. Cells never treated with hymeglusin exhibited a sigmoidal growth curve which exhibited an inflection point at 11.2 hours (Fig. 12). In contrast, pretreated cells that remained in hymeglusin containing medium never demonstrated any recovery in growth over the 36 hour experiment. Cells previously treated with hymeglusin prior to resuspension in medium without this inhibitor exhibited a lag before growth resumed. The inflection point in the growth curve for this sample was observed at 20 hours. The ability of inhibited cells to resume growth upon removal of hymeglusin from their medium is likely to reflect the slow endogenous hydrolase activity of HMGCS as demonstrated for other HMGCS enzymes (63). In the absence of a condensation reaction partner for the thioester bound moiety (in this case, ring-opened hymeglusin), solvent water reacts with the thioesterified moiety to release it as a hydrolysis product and the active site cysteine is liberated for a productive reaction. This slow process presumably accounts for the > 6 hour lag time before growth resumes after cells are pretreated with

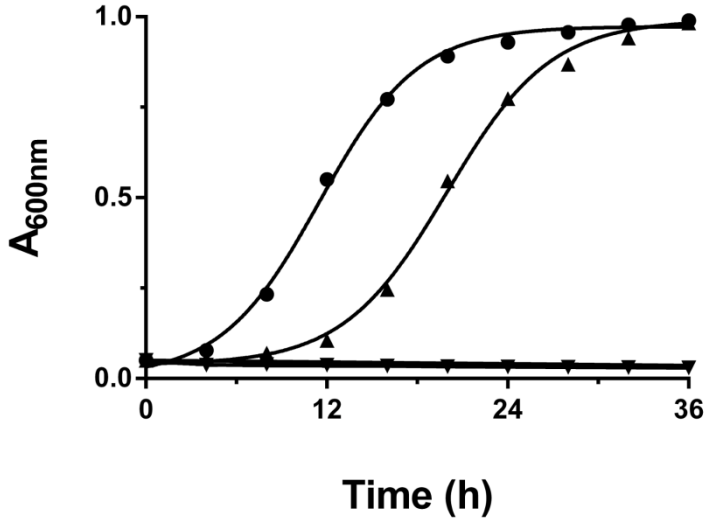

Figure 12. Hymeglusin inhibition and recovery of *H. volcanii* cellular growth. *H. volcanii* H1209 was grown in the presence or absence of hymeglusin in Hv-YPC media at 45^{o}C for 4 hours and pelleted by centrifugation. Cells were resuspended in Hv-YPC media in the presence or absence of hymeglusin and incubated at 45^{o}C and 200 rpm in a 24-well plate. Growth was monitored by absorbance at 600 nm. Plots depict *H. volcanii* H1209 (●) never grown in the presence of hymeglusin, (▲) grown in presence of hymeglusin only before resuspension, (▼) grown in the presence of hymeglusin before and after resuspension. Curves represent nonlinear regression fits of the data.

inhibitor, as reflected in the delay in reaching an inflection point for the growth curve of this sample. Thus, the sub-micromolar affinity of hymeglusin for purified *Hv*HMGCS (Fig. 11) as well the efficacy and selectivity of this inhibitor for this key enzyme of isoprenoid biosynthesis are useful in implicating the essentiality of both the enzyme and the pathway for propagation of *H. volcanii*.

Discussion

The recently developed overexpression system for halophilic proteins has allowed for the first isolation and characterization of an archaeal HMG-CoA synthase. While the protein expression levels are lower than traditional and commonly used expression systems, recovery of 1.5 milligrams of protein per liter proved sufficient purified protein for enzymatic characterization. The utilization of high-salt conditions during protein isolation also permit the production of stable, halophilic proteins that otherwise might denature in the low-salt conditions common with traditional expression systems. This advantage was demonstrated with the attempt to produce HMG-CoA synthase from *E. coli*. The experiment resulted in insoluble, inactive protein. The *H. volcanii* expression system also obviates the need for denaturing and refolding regimens and concern over loss of intrinsic physiological characteristics. The rationale outlined above prompted us to investigate *Haloferax* expression methodology to study enzymes of *Haloferax* isoprenoid biosynthesis.

The recovery of sufficient quantities of *Hv*HMGCS protein from a *H. volcanii* host allows for a convincing comparison of the archaeal form to other eukaryotic and bacterial forms of the enzyme. The K_m, V_{max}, and catalytic efficiency values for *Hv*HMGCS are quite similar to documented values for both the eukaryotic and bacterial enzyme. A noteworthy

contrast is the lack of substrate inhibition to acetoacetyl-CoA. Reported K_i values for acetoacetyl-CoA for *E. faecalis* and *H. sapiens* were 1.9μM and 12μM, respectively. This lack of substrate inhibition distinguishes *Hv*HMGCS from both the bacterial and eukaryotic enzyme. There are also clear differences in hymeglusin inhibition. While the experimentally determined K_i were similar, the k_{inact} values determined for hymeglusin against *Hv*HMGCS (17.3 min^{-1}) is much faster than either the *H. sapiens* (1.06 min^{-1}) or *E. faecalis* (3.5 min^{-1}) enzyme. These experiments also suggest that *Hv*HMGCS uses the same catalytic mechanism, and in particular the catalytic cysteine, as HMGCSs employed by eukaryotic and bacteria forms of the enzyme (26,80).

The inhibition of *Hv*HMGCS by hymeglusin prompted interest in its use to determine the essentiality of *Hv*HMGCS to *H. volcanii*. Incubation of *H. volcanii* cells in the presence of hymeglusin effectively blocked cellular propagation compared to cells not treated with hymeglusin. Recovery of cells treated with hymeglusin involves a substantial lag time for *Haloferax* (growth curve inflection point at 20 hours versus 11 hours for untreated control) and also a notable lag for *E. faecalis* (inflection point at 3.1 hr. versus 0.7 hr. for untreated control). For animal HepG2 cells, 50% recovery of HMGCS from hymeglusin inactivation occurs more rapidly (~1 hour) (81). These *in vivo* experiments confirm the essentiality of *Hv*HMGCS to *H. volcanii*. Since HMG-CoA synthase represents the first committed step of the pathway, these experiments also suggest that the mevalonate pathway is essential in the production of isoprenoids in *H. volcanii*.

The results of these experiments provide the first characterization of a HMG-CoA synthase from any archaeon. Reports of functional demonstrations of HMG-CoA reductases

(32,33,34) and mevalonate kinases (37,38,39) have been provided from other archaea. Phylogenetic analysis of many archaeal sequenced genomes has revealed the conservation of these enzymes across the entire domain (36). The characterization of these enzymes along with the reports of conservation reveals that the first half of the mevalonate pathway is intact in Archaea.

The terminal reactions of the mevalonate pathway in Archaea have remained unresolved. These reactions may be catalyzed by enzymes analogous to enzymes of the classical mevalonate pathway although the analysis of sequenced archaeal genomes has yet to identify the genes responsible. The discovery of an isopentenyl monophosphate kinase (IPK) from *M. jannaschii* (51) has prompted a competing hypothesis that Archaea may use an alternate route in mevalonate metabolism. However, analysis of sequenced archaeal genomes has yet to provide any indications of the missing enzyme(s) that would potentially complete the 'alternate' pathway. With the inability of bioinformatics to discover these missing enzymes, the expression and isolation of the *Haloferax* enzymes in their native state seems to represent the most reliable approach to pursue.

CHAPTER 4

DISCOVERY OF A PHOSPHOMEVALONATE DECARBOXYLASE AND THE ALTERNATE MEVALONTE PATHWAY IN *H. VOLCANII*

Introduction

The terminal reactions of the classical mevalonate (MVA) pathway are catalyzed by the enzymes phosphomevalonate kinase (EC 2.7.4.2) and mevalonate diphosphate decarboxylase (EC 4.1.1.33) (26). Phosphomevalonate kinase catalyzes the reversible phosphoryl transfer from ATP to mevalonate to produce mevalonate 5-phosphate. Mevalonate diphosphate decarboxylase catalyzes the ATP dependent decarboxylation of mevalonate 5-diphosphate to isopentenyl 5-diphosphate. These enzymes together produce isopentenyl diphosphate which is the precursor to the many biologically synthesized isoprenoid derived molecules (Fig. 13). Functional demonstrations of these enzymes have been widely documented from both the eukaryotic (82,83,84,85,86) and bacterial (86,87,87,88,89,90) domains of life.

Despite the identification of the terminal reactions in eukaryotes and bacteria and the knowledge that Archaea metabolize mevalonate, the terminal reactions of the MVA in archaea remain cryptic. Annotations to sequenced archaeal genomes suggest that, as a domain, archaea lack both a phosphomevalonate kinase and mevalonate diphosphate decarboxylase (36). There have been reports of the classical MVA pathway enzymes, phosphomevalonate kinase (PMK) and mevalonate diphosphate decarboxylase (MDD), in

operation in *Sulfolobus* (62). However, these enzymes do not represent how isoprenoids are largely synthesized in archaea as homologs to PMK and MDD have not been detected in any other archaeal genus (36). These classical MVA pathway enzymes also have been proposed to have been acquired from a lateral gene transfer from bacteria (50).

Recently, an enzyme was discovered in *M. jannaschii* that could represent one of the missing terminal mevalonate pathway enzymes. This enzyme, isopentenyl monophosphate kinase (IPK), utilizes isopentenyl monophosphate and ATP as a substrate producing isopentenyl diphosphate (51). The similarity of the substrates and the inability to find the classical terminal reaction enzymes suggested the possibility that Archaea use an alternate route to produce isopentenyl diphosphate (Fig. 13). In this alternate route, a decarboxylation would precede the phosphorylation catalyzed by isopentenyl monophosphate kinase. This would require the existence of a novel phosphomevalonate decarboxylase which has never been demonstrated to exist anywhere in nature.

To identify the enzymes responsible for the terminal reactions of the mevalonate pathway in archaea, open reading frames from the *H. volcanii* genome were candidate screened against known bacterial and eukaryotic versions of phosphomevalonate kinase, mevalonate diphosphate decarboxylase, and isopentenyl monophosphate kinase. Hits were selected for sub-cloning into plasmids suitable for overexpression in the *H. volcanii* host successfully used to isolate the previously described mevalonate pathway enzyme, HMG-CoA synthase. Recovery of active enzymes has now led to identification of a *H. volcanii* IPK and the monophosphate-specific phosphomevalonate decarboxylase (PMD). This

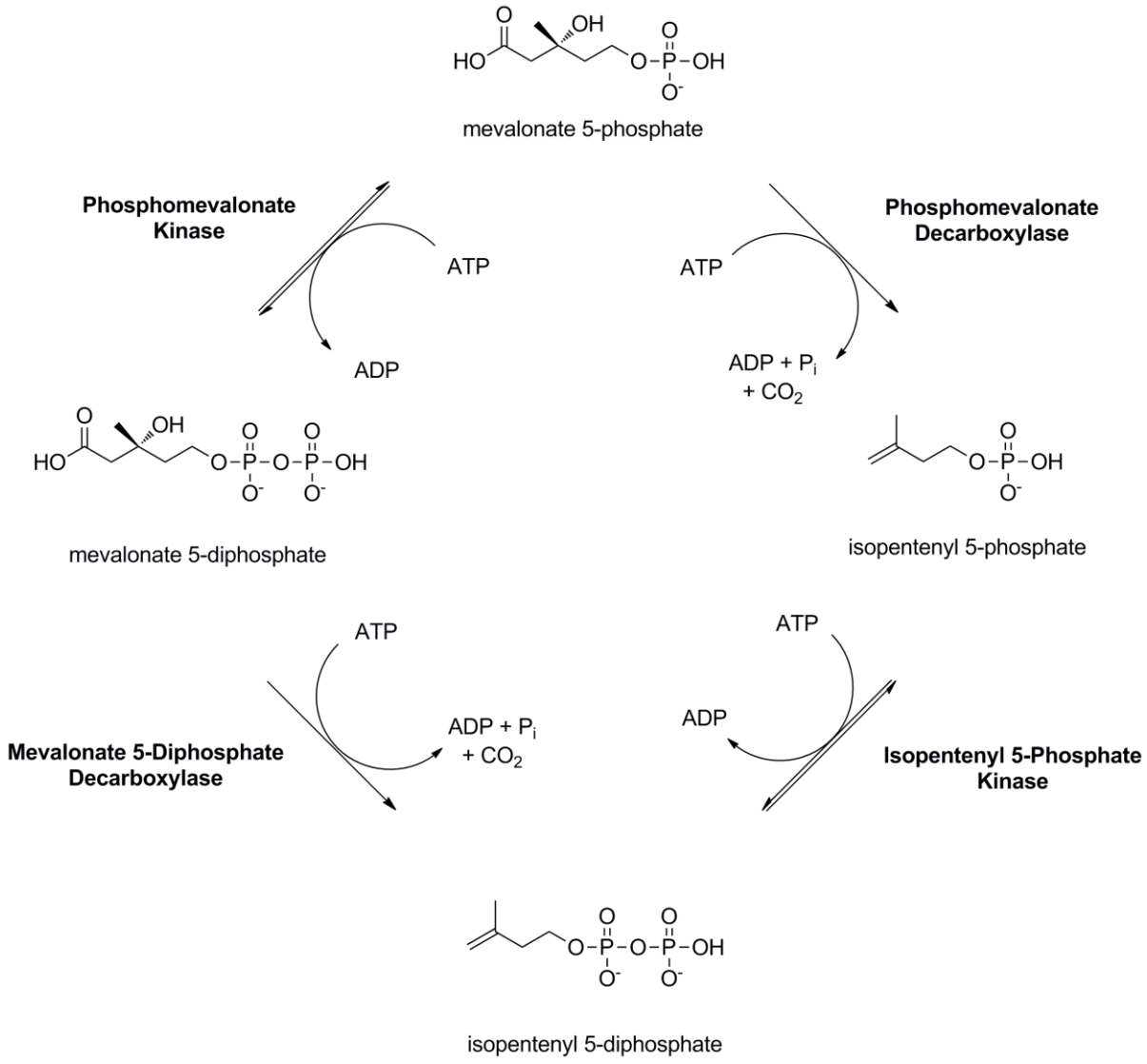

Figure 13. Terminal Enzyme Reactions of the Classical and Alternate Mevalonate Pathway**.** The enzymes that catalyze the terminal reactions of the classical mevalonate pathway, phosphomevalonate kinase and mevalonate diphosphate decarboxylase, are indicated on the left. The enzymes that catalyze terminal reactions of the alternate mevalonate pathway, phosphomevalonate decarboxylase and isopentenyl monophosphate kinase, are indicated on the right.

represents the first identification of any phosphomevalonate decarboxylase and the first experimental demonstration of the enzymes responsible for an alternate mevalonate pathway.

Results

Identification and Sequence Comparison of *Haloferax volcanii* HVO_1412 with Eukaryotic and Prokaryotic MDD Enzymes

The annotation of the *H. volcanii* genome provided no indication of the enzymes responsible for the terminal reactions of the MVA pathway. Since archaea organize some biologically related open reading frames into operons, genes surrounding previously described MVA pathway enzymes were explored. Genes adjacent to the previously described HMG-CoA synthase and HMG-CoA reductase, both separated from each other on the *H. volcanii* genome, did not seem like promising targets. An open reading frame (HVO_2762) downstream of mevalonate kinase (MK) contained some identity (~30%) to the isopentenyl monophosphate kinase described previously (51, 53). However, flanking open reading frames to MK and IPK did not present themselves as encoding obvious MVA pathway enzymes.

A BLAST and PSI-BLAST search was then performed against the *H. volcanii* genome as a database using bacterial and eukaryotic versions of PMK and MDD as queries. No homologs were detected for PMK using BLAST or PSI-BLAST against *H. volcanii*. However, an open reading frame (HVO_1412) with a low homology (~30% at the protein

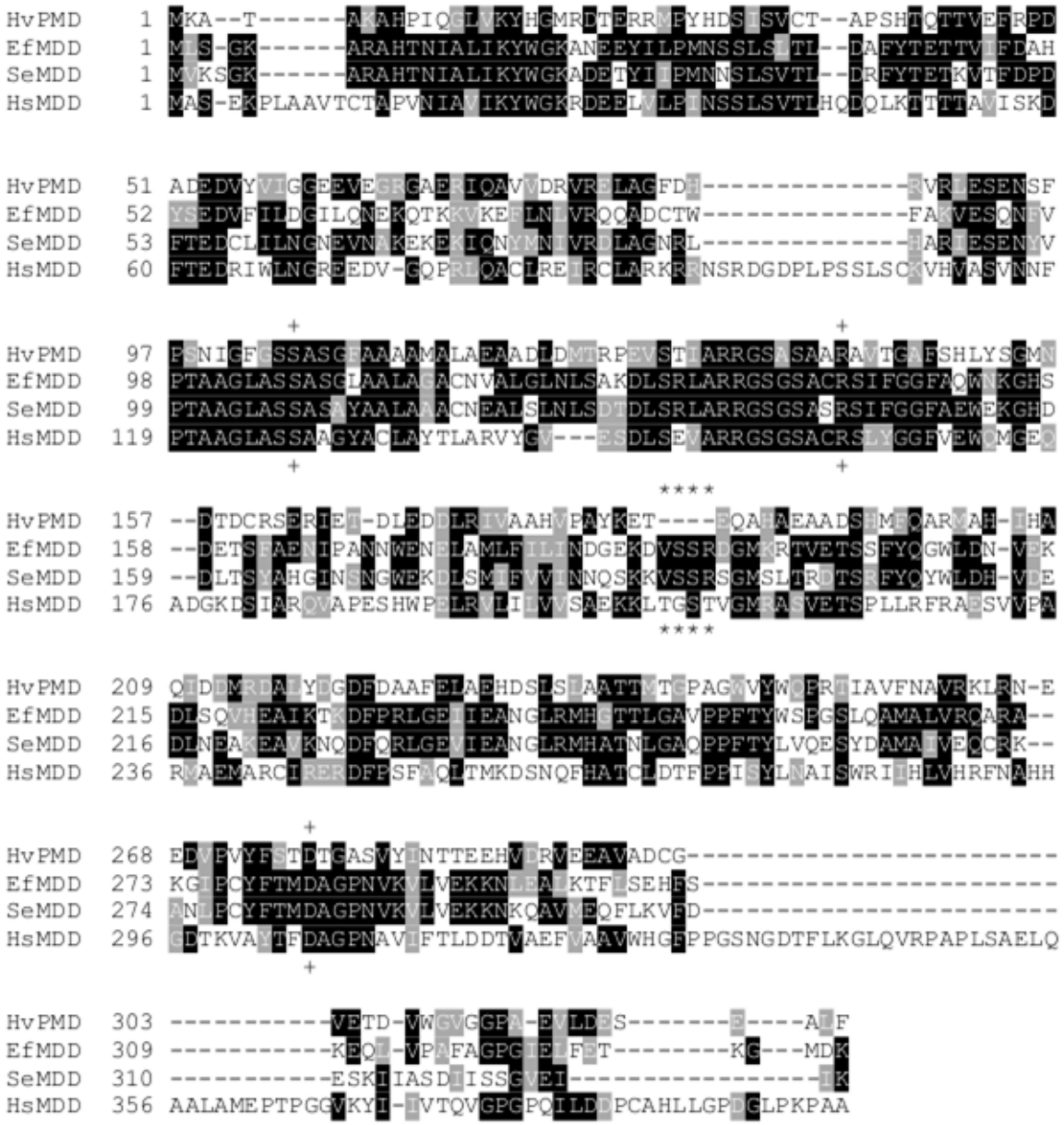

Figure 14. Multiple Sequence Alignment of Phosphomevalonate Decarboxylase.

Figure 14. Continued The sequence of phosphomevalonate decarboxylase from *H. volcanii* (*Hv*PMD) was aligned with mevalonate diphosphate decarboxylases from *E. faecalis* (*Ef*MDD), *S. epidermidis* (*Se*MDD) and *H. sapien*s (*Hs*MDD). Conserved residues are in black and similar residues are in gray. The PMD 'gap' is indicated with asterisks. Catalytically conserved residues are indicated with a plus. The alignment was performed by T-Coffee and visualized by Boxshade.

level) to *S. epidermidis* MDD presented itself as a potential mevalonate pathway enzyme (Fig. 14). The classical MDD enzyme is a GHMP kinase family protein and contains three residues critical to the decarboxylation of mevalonate 5-diphosphate (26). These residues, an aspartic acid, serine, and arginine, along with the ATP binding domain inherent to GHMP kinases appeared conserved in HVO_1412 (Fig. 14). While no potential homolog for PMK presented itself, the identification of an open reading frame that appeared to be a mevalonate 5-diphosphate decarboxylase prompted interest in its expression and characterization.

Expression and Substrate Specificity of *Hv*PMD

HVO_1412 was sub-cloned into pTA963, overexpressed in *H. volcanii* H1209 strains, and isolated by Ni-column chromatography. The protein was purified to apparent homogeneity (Fig. 15). SDS-page indicates a molecular mass (48.0 kDa) that is higher than the predicted mass of the His-tagged protein (37,304 Da). Anomalous SDS-page results are common with halophilic proteins and are attributed to the overabundance of acidic residues (76). The MALDI estimate of 37,328 ± 21 Da for this protein is in agreement with the predicted mass deduced from the sequence of the expressed protein.

The preferred substrate for this enzyme was determined by incubating the protein in the presence of various mevalonate pathway substrates. Activity was detected using the pyruvate kinase and lactate dehydrogenase coupled assay. This assay couples the utilization of 1 ATP to the oxidation of 1 NADH and can be monitored at A_{340}. The incubation of mevalonate and ATP with the protein yielded negligible activity with a calculated specific

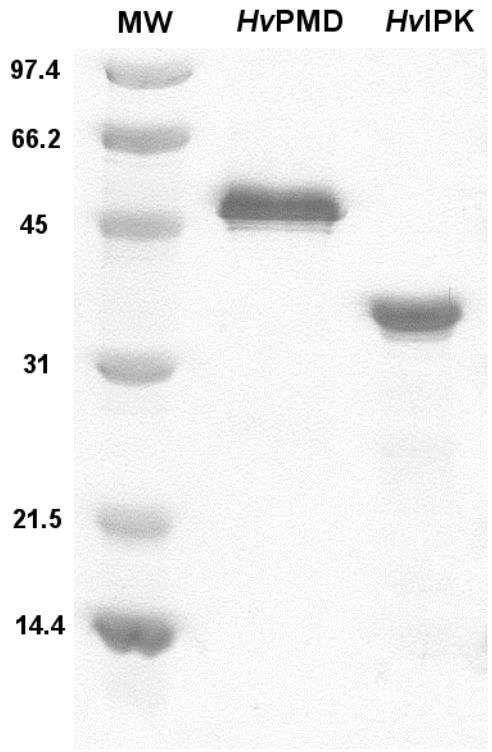

Figure 15. SDS-PAGE of Purified *Haloferax* Phosphomevalonate Decarboxylase and Isopentenyl Monophosphate Kinase**.** Left lane, molecular weight markers (kDa); center lane, phosphomevalonate decarboxylase (4 µg); right lane, isopentenyl monophosphate kinase (4 µg). Isopentenyl monophosphate kinase was provided by Rana Zalmai and Andrew Skaff.

activity of 0.004 U/mg. The same result was observed when the protein was incubated with mevalonate 5-diphosphate with a calculated specific activity of 0.004 U/mg. A surprising result was obtained with enzyme and mevalonate 5-P. In the presence of mevalonate 5-P and ATP, the enzyme reaction mixture exhibited substantial activity with a calculated specific activity of 4.8 U/mg. This represented a ~1,000x fold increase in activity compared to either mevalonate or mevalonate 5-diphosphate. The dramatic increase in activity strongly indicated that mevalonate 5-P and ATP are the substrates for this enzyme.

*Hv*PMD Salt Dependence, pH Dependence, and Kinetic Characterization

Enzyme characterization studies indicate that *Hv*PMD exhibits optimal catalytic activity at pH ~7.5 (Fig 16). This compares favorably to other classical mevalonate 5-diphosphate decarboxylases from the eukaryotic and bacterial domains. *Hv*PMD surprisingly exhibits activity that is not strongly dependent on salt concentration (Fig 17). While *Hv*PMD is substantially active at saturating levels of KCl, it is not significantly more or less active than with no salt. Substrate saturation experiments indicated a V_{max} = 5.6 U/mg for both mevalonate 5-P and ATP with a k_{cat} = 3.5 s^{-1} (Table 1, Fig 18).These values are also comparable to both bacterial (90) and eukaryotic MDD (61) enzymes (Table 1). K_m determination for (*R,S*)-mevalonate 5-phosphate and (*R*)-mevalonate 5-phosphate, 159µM and 75µM, respectively, show that *Hv*PMD utilizes only the (*R*) isomer consistent with previously documented mevalonate pathway enzymes (Table 1, Fig 18).

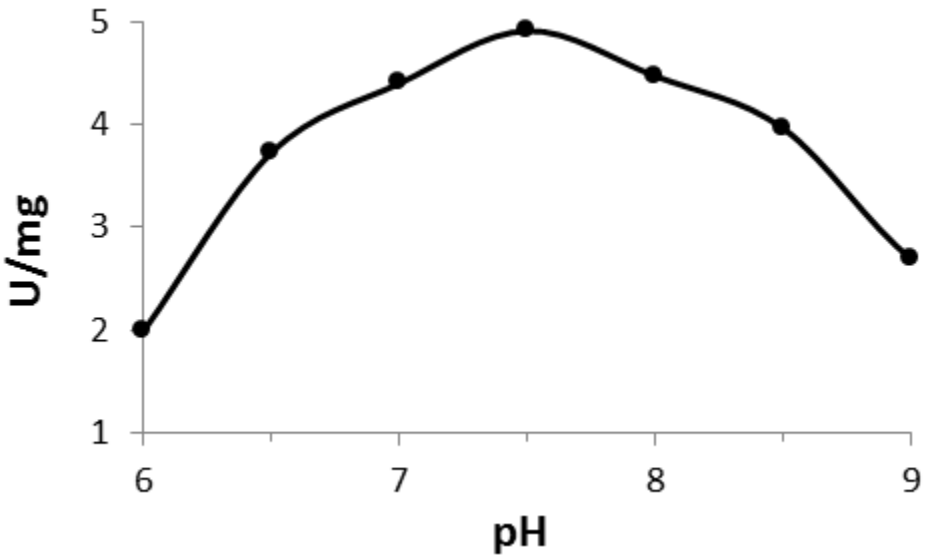

Figure 16. pH dependence of *Hv*PMD. Specific activity was measured by monitoring the disappearance of ADP at A_{340} using the pyruvate kinase / lactate dehydrogenase assay at saturating levels for both mevalonate 5-P (2mM) and ATP (2mM) at 30^{o}C. pH (●) ranged from 6 to 9, as indicated.

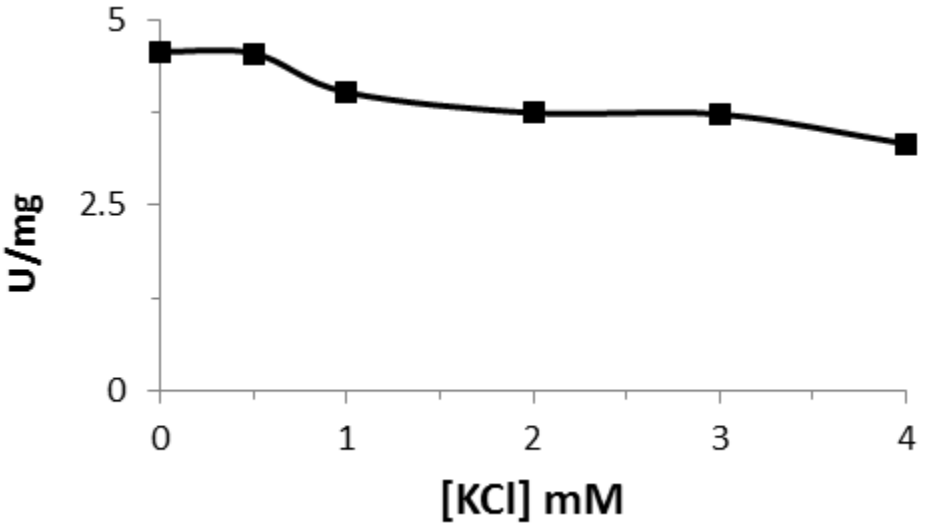

Figure 17. Salt Dependence of *Hv*PMD. Specific activity was measured by monitoring the disappearance of ADP at A_{340} using the pyruvate kinase / lactate dehydrogenase assay at saturating levels for both mevalonate 5-P (2mM) and ATP (2mM) in 50mM Tris-Cl, pH 7.5, at 30^{o}C. Concentrations of KCl (■) ranged from 0 to 4M, as indicated.

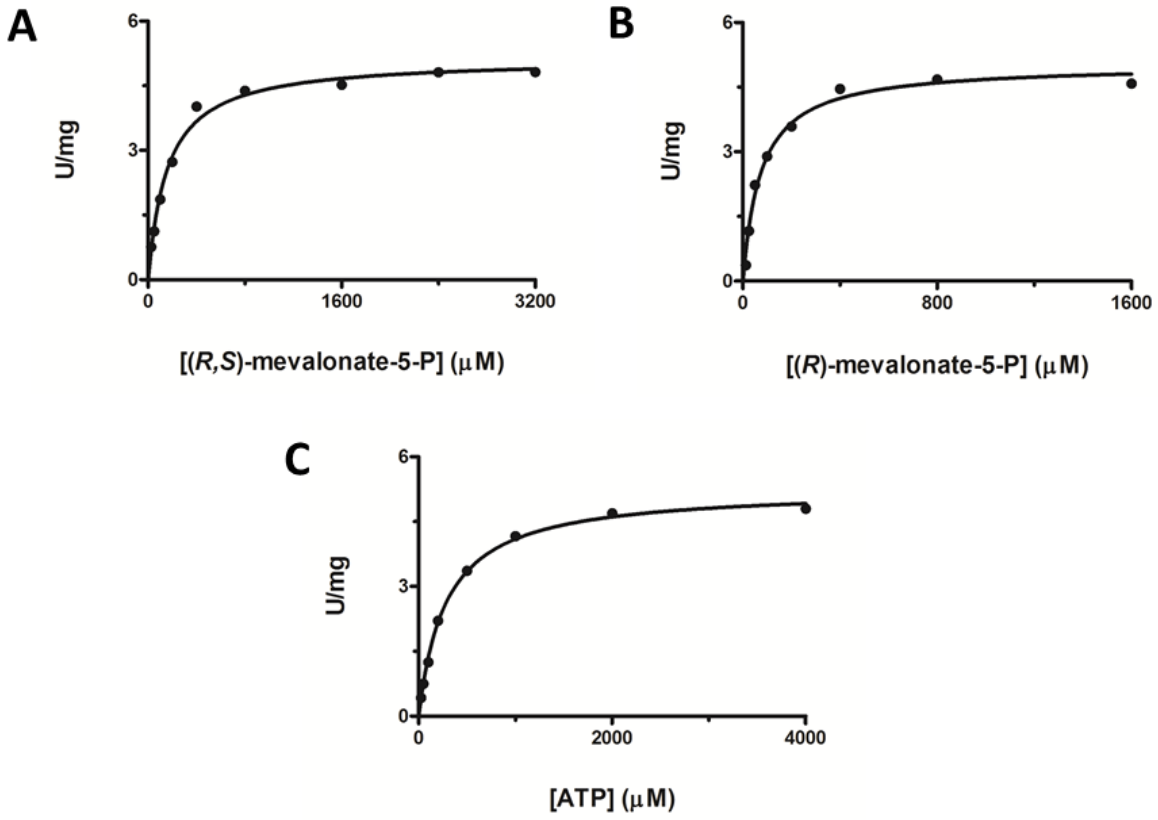

Figure 18. Dependence of *Hv*PMD Reaction Rates on Substrate. The specific activities of *Hv*PMD for (*R,S*)-mevalonate-5-P, (*R*)-mevalonate-5-P, and ATP were determined using the PK/LDH coupled assay at A_{340}. (A) *Hv*PMD assay with increasing (*R,S*)-mevalonate-5-P containing saturating ATP (2mM), (B) *Hv*PMD assay with increasing (*R*)-mevalonate-5-P containing saturating ATP (2mM). (C) *Hv*PMD assay with increasing ATP containing saturating (*R,S*)-mevalonate-5-P (2mM). Data points represent specific activities at the indicated concentrations of substrate and were analyzed with GraphPad 5.0.

Table 3. Kinetic constants for *H. volcanii* PMD, *S. epidermidis* MDD, and *H. sapiens* MDD

Parameter (units)	*H. volcanii* PMD[a]	*S. epidermidis* MDD[c]	*H. sapiens* MDD[d]
K_m (*R,S*)-mevalonate 5-P (μM)	159 ± 15[b]	N/A[e]	N/A[e]
K_m (*R,S*)-mevalonate 5-PP (μM)	N/A	9.1 ± 0.9	28.9 ± 3.3
K_m ATP (μM)	290 ± 15	27 ± 3	690 ± 70
V_{max} ($\mu molmin^{-1}mg^{-1}$)	5.6 ± 0.1	9.8 ± 0.3	6.1 ± 0.5
k_{cat} (s^{-1})	3.5 ± 0.1	5.9 ± 0.2	4.4 ± 0.4
k_{cat} / K_m ($s^{-1}M^{-1}$)	$(2.2 \pm 0.2)x10^4$	$(6.5 \pm 0.7)x10^5$	$(1.6 \pm 0.2)x10^5$

[a] values are means and standard errors.

[b] K_m for (*R*)-mevalonate 5-phosphate is 75 ± 8 μM.

[c] Data for *S. epidermidis* MDD were previously reported by Barta et al. (90)

[d] Data for *H. sapiens* MDD were previously reported by Voynova et al. (61)

[e] N/A , not applicable

Enzymatic and Mass Spectrometric Determination of the *Hv*PMD Reaction Product

With the substrates clarified and kinetic parameters determined, work towards identifying the product of this enzyme was attempted. Determining the chemical identity of the reaction product would be necessary to reveal the function of this enzyme. The first approach used to identify the product employed the use of a second ATP utilizing enzyme as a reporter. *Hv*PMD was incubated in the presence of mevalonate 5-P and ATP and the reaction was allowed to go to completion. The reporter enzyme then was added to the reaction and progress was monitored again. Since enzymes are specific for substrates, any activity monitored by the second reporter enzyme should reveal the product of HVO_1412. The first reporter enzyme used was the classical mevalonate pathway enzyme mevalonate 5-diphosphate decarboxylase from *S. epidermidis* (*Se*MDD). The addition of *Se*MDD failed to stimulate any additional activity from the reaction mixture. This suggested that the product of the first reaction, that included *Hv*PMD, mevalonate 5-P, and ATP, was not mevalonate 5-diphosphate. The utilization of human mevalonate kinase and phosphomevalonate kinase as the second reporter enzyme also yielded the same result. A surprising result was observed when isopentenyl monophosphate kinase from *H. volcanii* was used as the second reporter enzyme. After the addition of *Hv*IPK to the reaction mixture, substantial additional activity was detected. This strongly implicated isopentenyl 5-phosphate as the product of the enzymatic reaction catalyzed by *Hv*PMD. To confirm the results from the *Hv*IPK reporter experiment, an experimental test of reaction

Table 4. Enzymatic Identification of the PMD Reaction Product

A. Selectivity of PMD product metabolism by IPK or MDD			
R-MVA 5-P present in reaction mix (nmol)	51.1 ± 2.5	55.2 ± 0.1	
Product formation: PMD + IPK[a] added (nmol)	52.2 ±1.8	-	
Product formation: PMD + MDD[b] added (nmol)	-	2.0 ± 0.1	
B. Reaction stoichiometry			
(*R*)-MVA 5-P added (nmol)	25	50	75
*Hv*PMD reaction product formed (nmol)	24.6 ± 2.5	51.1 ± 3.6	74.9 ± 0.3
PMD reaction product utilized by *Hv*IPK (nmol)	24.7 ± 1.1	52.2 ± 1.8	76.5 ± 2.0
Reaction stoichiometry	1.01 ± 0.04	1.02 ± 0.01	1.02 ± 0.03

Table 4. Continued

Conversion of mevalonate 5-phosphate by PMD and subsequent ATP dependent conversion of the PMD reaction product (or any unreacted mevalonate 5-phosphate) by secondary enzymes (isopentenyl kinase, IPK or mevalonate diphosphate decarboxylase, MDD) was measured using the pyruvate kinase/lactate dehydrogenase coupled assay described in Methods.

[a] *H. volcanii* IPK (5 µg) was incubated with the PMD reaction product.

[b] *S. epidermidis* (20 µg) was incubated with the PMD reaction product.

stoichiometry was performed. Three different molar quantities of mevalonate 5-P were added to separate reaction mixtures with *Hv*PMD and ATP and the reaction allowed to go to completion. *Se*MDD or *Hv*IPK were added to the reaction mixtures and the reaction was again allowed to go to completion. The amount of the product from the first enzymatic reaction and the amount of the product from the second enzymatic reaction were quantified. As seen in Table 2, the addition of *Se*MDD failed to stimulate any activity at any concentration. This is in contrast to the complete metabolism of the reaction product by *Hv*IPK at every concentration. The ratio of the second product quantity to the first product quantity approached unity only for *Hv*IPK strongly suggesting that isopentenyl 5-phosphate was the product of *Hv*PMD.

Further support for the identity of the *Hv*PMD reaction product as isopentenyl 5-phosphate was obtained by mass spectrometry. *Hv*PMD was incubated in the presence of mevalonate 5-P and ATP. The product of the reaction was then isolated by anion exchange chromatography . The isolated product along with chemical standards were used for mass determination by ESI-MS (Fig. 19). Peaks for the chemical standards (*R,S*)-mevalonate 5-P and isopentenyl 5-phosphate were detected at their predicted masses, [$(M-H)^-$, m/z = 227]; and [$(M-H)^-$, m/z = 165], respectively. The negative control which contained only (*R,S*)-mevalonate 5-P and ATP showed a predicted peak at 227. Two peaks were observed in the positive control where *Hv*PMD was incubated with (*R,S*)-mevalonate and ATP. The two peaks were masses of 227 and 165 in nearly equal quantities. The emergence of a mass peak of 165 in the positive control corresponds to the mass of isopentenyl 5-phosphate (Fig. 19). The mass of 227 corresponds to unreacted (*S*)-mevalonate 5-P. These observations

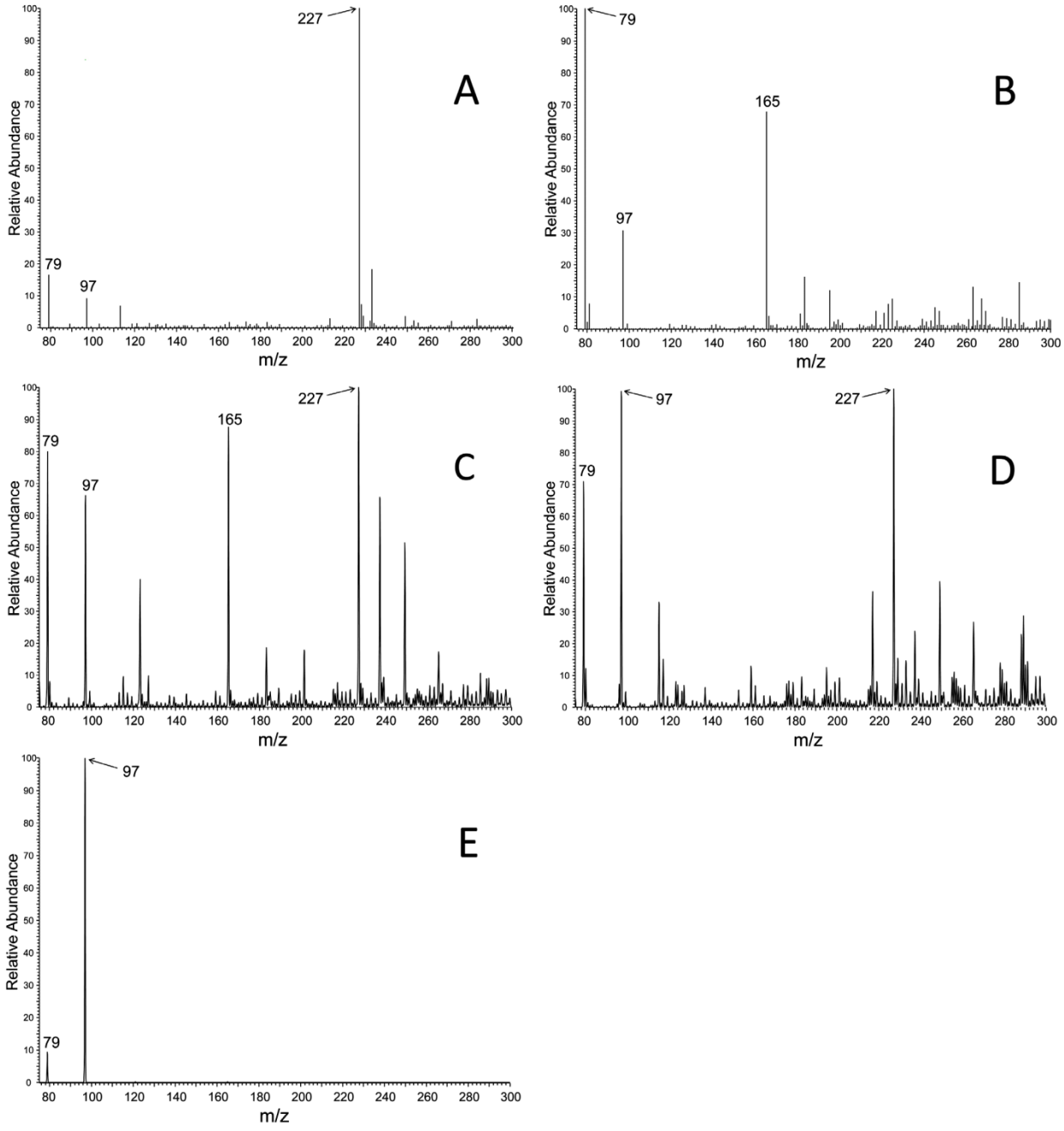

Figure 19. ESI-MS Analysis of Metabolites of the Phosphomevalonate Decarboxylase reaction.

Figure 19. Continued. All spectra were collected in the negative ion mode. Panel A. MS spectrum of chemically synthesized (*R,S*)-mevalonate 5-phosphate (m/z = 227). Panel B. MS Spectrum of chemically synthesized isopentenyl 5-phosphate (m/z = 165). C. MS Spectrum of a PMD reaction mixture indicating residual unreacted (*S*)-mevalonate 5-phosphate (m/z = 227) and showing product isopentenyl 5-phosphate (m/z = 165). D. MS Spectrum of negative control in which no enzyme is included in the reaction mix. Unreacted (*R,S*)-mevalonate 5-phosphate substrate is apparent (m/z = 227) but no formation of a product (m/z = 165) peak is observed. Panel E. MS/MS Spectrum of m/z = 635 165, yielding phosphate ions m/z = 79 and m/z = 97.

gave additional support that the identity of the product was, in fact, isopentenyl 5-phosphate. The collected results from both the stoichiometry and mass spectrometry experiments indicate that the product of *Hv*PMD is isopentenyl 5-phosphate and argue for the identity of this enzyme as a mevalonate 5-phosphate decarboxylase.

IC_{50} determination for (*R*)-fluoromevalonate 5-P and (*R*)-fluoromevalonate 5-PP Against *Hv*PMD

The assignment of this enzyme as a novel mevalonate 5-phosphate decarboxylase prompted an investigation into a potential inhibitor. The sequence similarity and conservation of critical residues between *Hv*PMD and the classical mevalonate pathway enzyme mevalonate 5-diphosphate decarboxylase (MDD) suggested they might share a common reaction mechanism. In this reaction, MDD uses ATP to activate the C3 hydroxyl into a leaving group by phosphorylation (91,92). This produces a carbocation at C3 that drives cleavage between C1 and C2 to form isopentenyl diphosphate (26). A potent inhibitor of MDD, 6-fluoromevalonate 5-PP, prevents the carbocation from forming and thus the decarboxylation. To determine if *Hv*PMD uses a similar reaction mechanism to mevalonate 5-diphosphate decarboxylase, *Hv*PMD was incubated in increasing concentrations of (*R*)-fluoromevalonate 5-P or (*R*)-fluoromevalonate 5-PP (Fig. 20) with ATP and the pyruvate kinase / lactate hydrogenase coupling system. The reaction was started with the addition of mevalonate 5-phosphate and the reaction progress was monitored at A_{340}. (*R*)-fluoromevalonate 5-PP was ineffective at inhibiting *Hv*PMD up to millimolar levels (Fig. 21). However, (*R*)-fluoromevalonate 5-P proved to be a strong inhibitor of *Hv*PMD with an IC_{50}

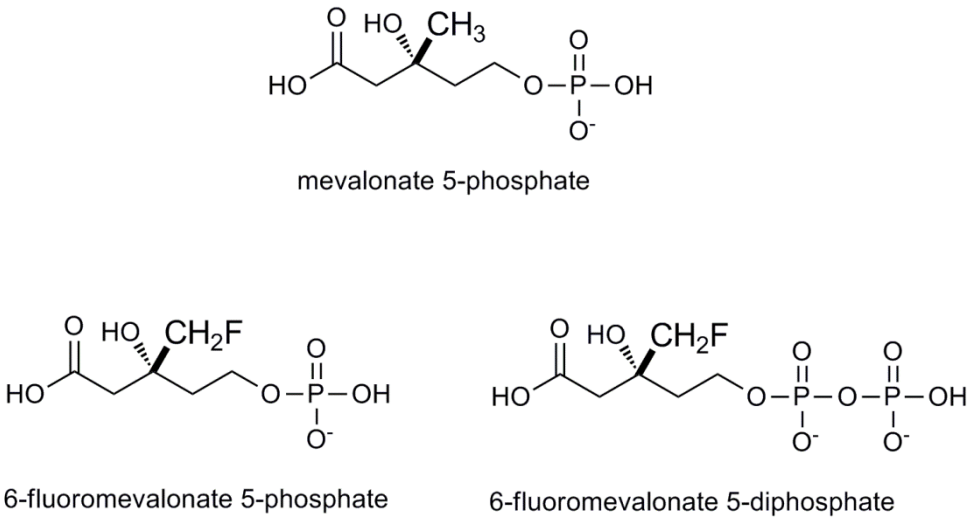

Figure 20. Mevalonate 5-Phosphate and Fluorinated Analogs.

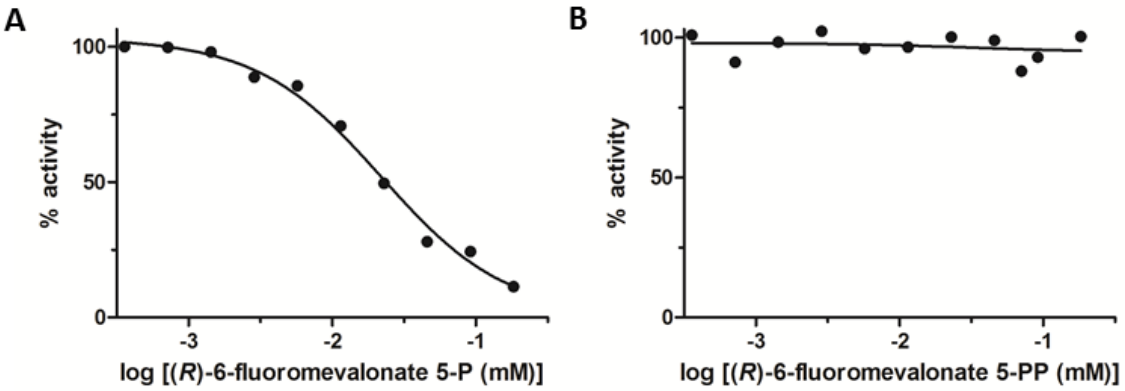

Figure 21. IC_{50} Determination for 6-fluoromevalonate 5-phosphate and 6-fluoromevalonate 5-diphosphate Against *Hv*PMD. Differential sensitivity of phosphomevalonate decarboxylase to inhibition by (A) 6-fluoromevalonate 5-phosphate and (B) 6-fluoromevalonate 5-diphosphate. Curves indicate an IC_{50} value of 16uM for the monophosphate containing inhibitor while the diphosphate containing compound exhibits no inhibition.

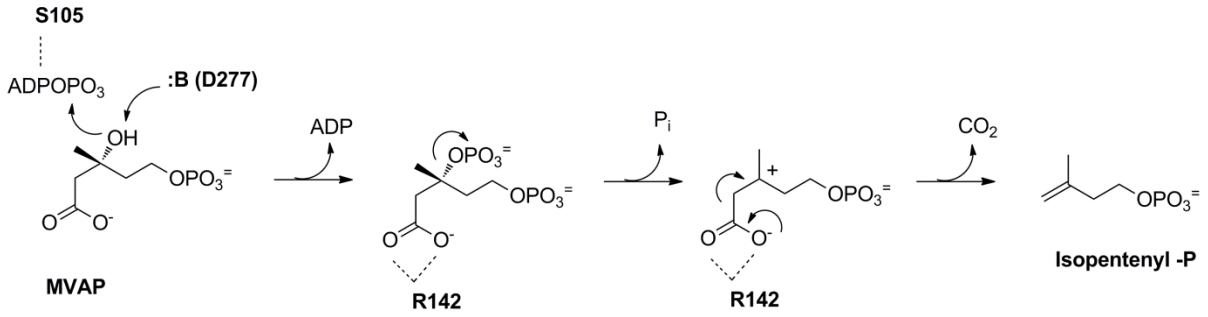

Figure 22. Proposed *Haloferax volcanii* Phosphomevalonate Decarboxylase Reaction Mechanism. Potential roles of active site residues serine-105, arginine-142, and aspartate-277 in substrate binding and catalysis.

value of 16μM (Fig. 21). The observed inhibition of *Hv*PMD by (*R*)-fluoromevalonate 5-P suggests that *Hv*PMD uses a similar reaction mechanism employed by the classical mevalonate pathway enzyme MDD. The details of this proposed mechanism involve a D277 acting as a general base to support the formation of a 3-phospho intermediate, a carbocation formation at C3 when the phosphoryl group leaves, with R142 supporting cleavage of C1 (Fig. 22). The surprising result is that *Hv*PMD is selective for the monophosphorylated inhibitor further indicating its selectivity for monophosphorylated compounds.

Discussion

The development of plasmids and host strains suitable for the overexpression of archaeal proteins has allowed for a broader investigation into isoprenoid biosynthesis in *H. volcanii*. This investigation has provided clarity to the terminal reactions and provided a demonstration of the enzymes responsible for an alternate mevalonate pathway. The report that the *M. jannaschii* genome encoded an isopentenyl monophosphate kinase (IPK) suggested the operation of an alternate route in the terminal reactions of the mevalonate pathway (51). Subsequent functional demonstrations of the enzyme from *Thermoplasma* and the detection of conservation of IPK across the entire archaeal domain prompted the hypothesis that these microbes may use an alternate route in mevalonate metabolism (53). The apparent contradiction provided by the genome annotation of *H. volcanii* suggested the existence of the potential alternative pathway enzyme IPK (HVO_2762) and the classical pathway enzyme mevalonate diphosphate decarboxylase (HVO_1412) prompted interest in expression of both open reading frames. It is now clear, based on the experimental results,

that *H. volcanii* encodes both an IPK and a novel phosphomevalonate decarboxylase (PMD). These enzymes, in concert, provide a direct route for the terminal reactions and support the existence of an alternate mevalonate pathway.

The overexpression and isolation of the protein encoded by HVO_1412 from *H. volcanii* in *H. volcanii* allows a credible assignment of the open reading frame as a PMD. The enzyme is selective for monophosphorylated substrates as demonstrated by its considerable activity in the presence of mevalonate 5-P compared to both mevalonate and mevalonate 5-PP. The V_{max} and catalytic efficiency for *Hv*PMD with mevalonate 5-P and ATP compare favorably to values for diphosphate specific versions of the enzyme (Table 3). The selectivity of *Hv*PMD for monophosphorylated compounds was reinforced as (*R*)-fluoromevalonate 5-P proved to be a potent inhibitor (IC50= 16 µM) compared to (*R*)-fluoromevalonate 5-PP which itself exhibited no inhibition (Fig. 21). This selectivity for monophosphorylated mevalonate compounds instead of diphosphorylated compounds strongly argues for this assignment as a PMD. The identification of the reaction product as isopentenyl monophosphate by both a second enzyme reporter, *Hv*IPK, and mass spectrometry proves this enzyme facilitates decarboxylation of mevalonate 5-P. The inhibition experiments suggest that *Hv*PMD uses a similar reaction mechanism to classical MDDs. (*R*)-fluoromevalonate 5-PP is a potent inhibitor of classical MDDs as the fluorinated analog interferes with the removal of the 3-phospho group and formation of the carbocation (91,92). While (*R*)-fluoromevalonate 5-PP supported no inhibition, (*R*)-fluoromevalonate 5-P proved to be a potent inhibitor and likely interfered with the same catalytic mechanism employed by classical MDDs. The preference of monophosphorylated

mevalonate, identification of the product as isopentenyl monophosphate, and inhibition by fluorinated substrate analogs supports the assignment of HVO_1412 as a PMD.

A rationale for the substrate selectivity and catalytic mechanism is suggested by a scrutiny of the sequence alignments of *Hv*PMD against bacterial and eukaryotic MDDs. The alignment indicates good identity with the conservation of three catalytic residues critical to the chemistry of decarboxylation of mevalonate seen in MDDs. The catalytic base involved in forming a transient 3-phosphomevalonate 5-phosphate intermediate, D277, is conserved in *Hv*PMD (93,94). The residue, R142, which contains the guanidinium moiety that interacts with the C1 carboxyl to support decarboxylation when the 3-phospho group leaves generating a transient carbocation at C3, is also present in *Hv*PMD (61). A conserved serine, S105, responsible for interaction with ATP (61) is also conserved in *Hv*PMD. The inhibition observed by (*R*)-fluoromevalonate 5-P also supports the position that this enzyme utilizes the same catalytic mechanism as classical MDDs. While these conserved residues support a catalytic mechanism similar to that employed by traditional MDDs, they do not explain the monophosphorylated compound selectivity. The proposed four residue gap between *Haloferax* PMD T186 and E187 seems like a possible explanation. This gap omits a serine and arginine residue that have been implicated in making multiple interactions to the beta phosphate of mevalonate diphosphate in diphosphate specific MDDs. This gap represents a significant active site architectural change and may be responsible for monophosphoryl selectivity. In the context of the absence of these residues in the PMD “gap”, it will be interesting to determine whether, in other archaea that encode an IPK enzyme, there are also proteins annotated as MDD enzymes while functioning as PMD enzymes.

CHAPTER 5

CONCLUSIONS AND FUTURE DIRECTIONS

The development of tools for robust investigation into the proteins from domain Archaea has lagged behind the other two domains. This can be explained partially by the extreme nature of these organisms. The archaeal domain is overrepresented by species that have specialized for growth in conditions of extreme temperature, pressure, acidity, and salinity. Many of these archaea even require specialized facilities to culture. The establishment of a model organism amenable to easy culturing and genetic manipulation would facilitate experiments into the third domain.

Without an obvious archaeal model organism available for study, the recent development of plasmids and host strains suitable for overexpression of native, archaeal halophilic proteins in a *Haloferax* host appeared to offer a productive method to study enzymes responsible for isoprenoid biosynthesis in *H. volcanii* (55). The proteins expressed are His-tagged which facilitates isolation by Ni-column chromatography under high-salt conditions (>2M KCl) that the proteins generally require for proper folding. Protein can be isolated to near homogeneity on the Ni-column alone with some effort. The yield from this expression system is generally one mg per liter culture. While this quantity is lower than traditional expression systems such as *E. coli*, it is adequate for a large number of enzymatic experiments. Improvements in both total cell density and level of protein expressed may lead to quantities amenable for structural studies. The observation that an increase in cell

density and overall protein production can be achieved from an increase in media and longer growth times (data not shown) suggests there is untapped potential for this expression system.

The advantage to this approach over traditional approaches can be seen in the attempt briefly described in Chapter 3 to express HMG-CoA synthase from *H. salinarum* and *H. volcanii* in *E. coli*. Only insoluble and inactive protein was recovered (data not shown). This result is frequently encountered when proteins from a halophile are expressed in a traditional expression system. Archaeal halophiles have adapted to live in high salt by importing salt into the cytoplasm to match the environment. The proteins from archaeal halophiles have then adapted to operation in conditions of high salt. When these proteins are expressed in a traditional expression system under low salt conditions, these proteins improperly fold and are inactive. Active protein can occasionally be recovered using denaturing and renaturing protocols but these approaches are not always successful. This expression system obviates those concerns by providing the capability to produce native, halophilic proteins under high-salt conditions.

The results of the experiments utilizing these tools detailed in this account provide, for the first time, the missing enzymes responsible for mevalonate metabolism in *H. volcanii*. The *H. volcanii* genome encodes an HMG-CoA synthase. Kinetic characterization of *Hv*HMGCS reveals negligible differences in both substrate saturation and catalytic efficiency compared to eukaryotic and bacterial forms of the enzyme. However, *Hv*HMGCS is unique in that it is insensitive to substrate inhibition by acetoacetyl-CoA. This is in contrast to both bacterial and eukaryotic HMGCSs. For example, *E. faecalis* MvaS exhibits strong substrate

inhibition with a calculated K_i of 1.9μM for acetoacetyl-CoA (64). Substrate inhibition for acetoacetyl-CoA has also been reported for both yeast and human HMGCSs with a K_i of 8 μM and 12 μM, respectively (66,80). The biological function of this lack of substrate inhibition is unknown and additional demonstrations from other archaea would be useful in making any definitive claim regarding its importance. However, the difference in substrate inhibition of bacterial and eukaryotic HMGCS compared to the archaeal enzyme described here may be explained by the differences in the ultimate goal of the MVA pathway in these organisms. Archaea use the MVA pathway and HMGCS in particular to commit acetate to the production of large quantities of phytanic acid which is used in lipid membrane biosynthesis. During periods of growth any constraint may be undesirable. Eukaryotes and bacteria, in contrast, utilize the MVA pathway primarily to synthesize a large number of distinct, essential molecules of limited quantity. Substrate inhibition of HMGCS in bacteria and eukaryotes may then reserve acetate for other metabolic and biosynthetic pathways when the MVA pathway is not in operation.

Reports of the identification of an isopentenyl monophosphate kinase inspired the hypothesis that Archaea may utilize an alternate route in the terminal reactions of the mevalonate pathway. In this route, a decarboxylation would precede a phosphorylation catalyzed by IPK. Functional demonstrations of IPK have been provided from several archaea and conservation of the enzyme has been demonstrated in virtually every genome in the archaeal domain (36,51,52,53,54). This work also describes the recent characterization of an IPK from *H. volcanii* (95). The potential of an alternate MVA route, especially if catalyzed by enzymes with unique functions would explain why the terminal

reactions have remained elusive. However, the existence of an IPK did not prove the existence of an alternate route. Additional enzyme(s) that could provide a direct route to IP would be needed as experimental proof of an alternate route.

This proof was provided by the observation that the *H. volcanii* genome also encodes (HVO_1412) a novel phosphomevalonate decarboxylase (PMD). The expression of the HVO_1412 open reading frame in the *H. volcanii* expression system yielded an enzyme that supported robust decarboxylation activity for mevalonate 5-phosphate as compared to both mevalonate and mevalonate 5-diphosphate. Any ambiguity about its function was eliminated by both the enzymatic secondary reporter experiment and the mass spectrometry that both positively identified the product of the reaction as isopentenyl monophosphate. Thus, the protein encoded by HVO_1412 exhibits the functions expected for a phosphomevalonate decarboxylase (PMD) and joins the isopentenyl monophosphate (IPK) to complete the demonstration of an alternate MVA pathway in *Haloferax*.

The open reading frame that encodes this enzyme was identified because it shared significant protein sequence conservation to the classical mevalonate pathway enzyme mevalonate 5-diphosposphate decarboxylase (MDD). MDD is part of the GHMP kinase protein family, employs a conserved ATP binding domain, and contains three residues critical to the decarboxylation of mevalonate 5-PP. These residues include a serine that ligands to ATP, an aspartic acid that is the catalytic base responsible for forming a transient 3-phosphomevalonate 5-phosphate intermediate, and an arginine residue that contains the guanidinium moiety that interacts with the C1 carboxyl to support decarboxylation when the 3-phospho group leaves, generating a transient carbocation at C3 (93,94). These

residues are conserved in both the bacterial and eukaryotic MDDs and aligned well to corresponding residues in PMD (HVO_1412) at S105, D227, and R142 (61,93,94).

Given the large amount of conservation at the protein level and the similarity of substrates and products, it seemed reasonable to speculate that PMD used the same reaction chemistry as classical MDD enzymes. The reaction chemistry employed by MDD is vulnerable to fluorinated substrate analogs. For example, 6-fluoromevalonate 5-PP is an effective MDD inhibitor because the 3-fluoromethyl group interferes with the reaction chemistry by preventing the methyl group on C3 from donating the electrons needed to stabilize the transient carbocation at C3 of mevalonate 5-PP (60). Without this carbocation, there is no electron sink to drive the decarboxylation (60). 6-fluoromevalonate 5-P (IC50 = 16μM) proved to be an inhibitor of PMD. The results of the inhibition experiments using 6-fluoromevalonate 5-P strongly indicate that PMD uses the same catalytic mechanisms as other classical MDDs. In this reaction mechanism, the proposed mechanism is that the C3 hydroxyl group is converted to improved phosphate leaving group that results in the carbocation at C3 that provides the electron sink to drive the decarboxylation at C1.

The results from the inhibition experiments provided more than just the suggestion of the PMD reaction chemistry. PMD was shown to prefer monophosphorylated substrates. The preference of PMD for monophosphorylated substrates was reinforced when the monofluorinated substrate analog 6-fluoromevalonate 5-P proved to be a strong inhibitor (IC50 = 16 μM) while the diphosphorylated compound 6-fluoromevalonate 5-PP exhibited no inhibition. This is in contrast to the inhibition seen in MVA metabolism in eukaryotes and bacteria. 6-fluoromevalonate 5-PP has been demonstrated to be an effective MDD inhibitor

from enzymes from both the bacterial and eukaryotic domain. 6-fluoromevalonate 5-P had never been previously demonstrated to be an inhibitor of any enzyme. This is because 6-fluoromevalonate 5-P is the fluorinated analog to the substrate for the classical enzyme phosphomevalonate kinase (PMK). PMK uses an entirely different catalytic mechanism that isn't vulnerable to the same fluorinated substrate analogs.

The monophosphoryl selectivity exhibited by PMD despite sharing some sequence homology and active site residues to MDDs may be explained by the PMD 'gap'. While there is no direct experimental evidence for *Hv*PMD, the proposed four residue gap (as compared to the bacterial sequence) between T186 and T187 might account for the preference of PMD for monophosphorylated ligands. This gap omits a serine and arginine in the active site that has been shown to make multiple interactions to the beta phosphate of mevalonate 5-PP (90). The lack of these residues may represent a large active site change and be responsible for this enzyme's selectivity. It would be interesting to determine if deletion of these four residues could confer mevalonate 5-P selectivity to classical MDDs or if the addition of residues could confer mevalonate 5-PP selectivity to PMD. Structural studies of PMD would also be useful in determining the role of this gap, if any.

There is considerable interest in how or why the alternate pathway developed in *H. volcanii*. Kinetic comparisons between the enzymes of the classical and alternate pathway provide no obvious metabolic or chemical advantage to either route. The catalytic efficiency of enzymes responsible for either the terminal reactions of the classical or alternate route are very comparable as they approach or are in the 10^5 range. An increase in the K_m values for both IPK and PMD are noted compared to PMK and MDD. However, the larger K_m values

may only be *H. volcanii* specific or may represent an increase in carbon flux through the pathway for lipid biosynthesis rather than a particular catalytic benefit. The characterization of additional PMDs from other archaea and metabolomic studies into archaeal lipid biosynthesis would be useful in providing clarity to whether there is a catalytic benefit to the alternate or classical route.

The absence of an obvious metabolic or chemical advantage suggests that the development of an alternate mevalonate pathway may need to be explained by evolutionary biology. There are several rationales to suggest how this may have happened. One of these possibilities is that classical and alternate MVA pathways were present together in organisms ancestral to archaea, bacteria, and eukaryotes. Specialization of these pathways in these organisms may have led to pathways that now exist distinctly in each. Another hypothesis is that horizontal gene transfer can explain the diversity seen in isoprenoid biosynthesis in each domain. Bacteria may have acquired the MVA pathway from a eukaryote or perhaps an archaeaon. Archaea may have obtained an MDD from either bacteria or eukaryotes and specialization of that ancestral enzyme led to the PMD specificity. This specialization may be even seen to include the PMD 'gap' described previously.

The goal of this work was to discover the missing enzymes responsible for mevalonate metabolism in Archaea. *Haloferax volcanii* was chosen as the model organisms for this study because it is readily cultivable and newly developed expression plasmids and strains offered the possibility to express MVA pathway enzymes in their native physiological environment. The first half of the mevalonate pathway is catalyzed by HMG-CoA synthase,

HMG-CoA reductase and mevalonate kinase. Examples of archaeal HMG-CoA reductase and mevalonate kinases have been provided from a number of archaea, notably *M. jannaschii, S. solfataricus,* and *H. volcanii.* Analyses of archaeal genomes suggest that these enzymes are present in members of the entire domain. Homologs to the classical MVA pathway enzyme HMG-CoA synthase have also been proposed to be conserved. The details of this account provide, for the first time, the functional demonstration of an archaeal HMG-CoA synthase. The confirmation that this annotation was correct in *H. volcanii* gives support to the proposal that HMG-CoA synthase is conserved across the archaeal domain. It also supports the proposal that archaea produce mevalonate from acetate in the same manner as seen in bacteria and in eukaryotes.

The discovery that *H. volcanii* encodes both an IPK and PMD provides an account for the terminal reactions of the MVA pathway in this halophile. These enzymes together represent an alternate route in the terminal reactions in mevalonate metabolism. After this observation was made, it seemed reasonable to determine if these results represent mevalonate metabolism in all Archaea. IPK has been characterized from a number of archaea (52,53,54). The enzyme has also been detected in the genomes of virtually every archaea thus far examined (36).

Notable exceptions are *Metallosphera, Sulfolobus,* and *Nanoacchaeum*. The results from *Nanoacchaeum* can be ignored as its genome contains no homologs to MVA pathway enzymes (36). It has been proposed that *Nanoacchaeum* obtains its lipids from its obligate symbiont *Ignicoccus* which does have an IPK*. Metallosphera* and *Sulfolobus,* both from the order Sulfolobales from phylum Crenarchaeota, are exceptions as well as they contain the

only known archaeal homologs to the classical mevalonate pathway enzyme, phosphomevalonate kinase (36). The PMK from *Sulfolobus* has demonstrated to function with a classical MDD (49).

Excluding *Metallosphera , Sulfolobus,* and *Nanoacchaeum*, the *Hv*PMD sequence and the presence of the PMD 'gap' were used as a test to determine if PMD was conserved in Archaea. Potential homologs to *Hv*PMD can be detected in many archaea using BLAST and PSI-BLAST. As expected, PMD is strongly conserved among archaeal halophiles and representatives of the order Thermoplasmatales from the phylum Euryarchaeota. Homologs with low identity can be seen in other representatives in Euryarchaeota. This suggests that Euryarchaeota *may* use a PMD of the GHMP kinase family in an alternate route in MVA metabolism. However, no homologs to *Hv*PMD could be detected in Crenarchaeota. These observations can be interpreted to mean that since homologs to IPK are present in archaeal genomes from both Crenarchaeota and Euryarchaeota and considered conserved across the domain (36), that the discovery here of a PMD and IPK together in the *H. volcanii* genome implicates IPK as an alternate MVA pathway enzyme, then archaea, as a domain, likely use the alternate mevalonate pathway.

There are a number of potential explanations for the inability to detect PMD homologs in Crenarchaeota. The most reasonable is that archaea from Crenarchaeota encode a phosphomevalonate decarboxylase that isn't a GHMP kinase family protein. Such an observation would not be unprecedented. While most terminal MVA pathway enzymes are GHMP kinase family proteins, some are not. For instance, human PMK is part of the NMP kinase family (96,97). The details of this putative PMD enzyme may still include the

same catalytic mechanism seen in both MDDs and PMDs. The chemistry could also potentially be entirely unique. There is also the possibility that there is even a larger amount of metabolic diversity in the archaeal MVA pathway besides the alternate route described here. Progress towards identifying mevalonate metabolites and the isolation and characterization of additional PMDs from the third domain of life would be useful in evaluating these hypotheses.

REFERENCES

1. **Woese, C. R., and G. E. Fox.** 1977. Phylogenetic structure of the prokaryotic domain: the primary kingdoms. Proc Natl Acad Sci U S A **74:**5088-90.
2. **Woese, C. R., O. Kandler, and M. L. Wheelis.** 1990. Towards a natural system of organisms: proposal for the domains Archaea, Bacteria, and Eucarya. Proc Natl Acad Sci U S A **87:**4576-9.
3. **Dennis, P. P.** 1986. Molecular biology of archaebacteria. J Bacteriol **168:**471-8.
4. **Jarrell, K. F., A. D. Walters, C. Bochiwal, J. M. Borgia, T. Dickinson, and J. P. Chong.** 2011. Major players on the microbial stage: why archaea are important. Microbiology **157:**919-36.
5. **Allers, T., and M. Mevarech.** 2005. Archaeal genetics - the third way. Nat Rev Genet **6:**58-73.
6. **Reeve, J. N.** 2003. Archaeal chromatin and transcription. Mol Microbiol **48:**587-98.
7. **Huet, J., R. Schnabel, A. Sentenac, and W. Zillig.** 1983. Archaebacteria and eukaryotes possess DNA-dependent RNA polymerases of a common type. EMBO J **2:**1291-4.
8. **Aravind, L., and E. V. Koonin.** 1999. DNA-binding proteins and evolution of transcription regulation in the archaea. Nucleic Acids Res **27:**4658-70.
9. **Benelli, D., and P. Londei.** 2011. Translation initiation in Archaea: conserved and domain-specific features. Biochem Soc Trans **39:**89-93.

10. **Schafer, G., M. Engelhard, and V. Muller.** 1999. Bioenergetics of the Archaea. Microbiol Mol Biol Rev **63:**570-620.

11. **DeLong, E. F., and N. R. Pace.** 2001. Environmental diversity of bacteria and archaea. Syst Biol **50:**470-8.

12. **Jones, W. L., JA. Mayer, F. Woese, CR. Wolfe, RS.** 1983. *Methanococcus jannaschii* sp. nov., an extremely thermophilic methanogen from a submarine hydrothermal vent. Archives of Microbiology **136:**254-261.

13. **Zillig, W. S., KO. Wunderl, S. Schulz, W. Priess, H. Scholz, I.** 1980. The *Sulfolobus*-"Caldariella" Group: Taxonomy on the Basis of the Structure of DNA-Dependent RNA Polymerases Archives of Microbiology **125:**259-269.

14. **Elazari-Volcanii, B.** 1943. Bacteria in the Bottom Sediments of the Dead Sea. Nature **152:**274-275.

15. **Ferrer, M., O. V. Golyshina, A. Beloqui, P. N. Golyshin, and K. N. Timmis.** 2007. The cellular machinery of *Ferroplasma acidiphilum* is iron-protein-dominated. Nature **445:**91-4.

16. **Futterer, O., A. Angelov, H. Liesegang, G. Gottschalk, C. Schleper, B. Schepers, C. Dock, G. Antranikian, and W. Liebl.** 2004. Genome sequence of *Picrophilus torridus* and its implications for life around pH 0. Proc Natl Acad Sci U S A **101:**9091-6.

17. **Takai, K., K. Nakamura, T. Toki, U. Tsunogai, M. Miyazaki, J. Miyazaki, H. Hirayama, S. Nakagawa, T. Nunoura, and K. Horikoshi.** 2008. Cell proliferation at 122 degrees C and isotopically heavy CH4 production by a hyperthermophilic methanogen under high-pressure cultivation. Proc Natl Acad Sci U S A **105:**10949-54.

18. **Wolfe RS.** 2011. Techniques for cultivating methanogens. Methods Enzymol. **494**:1-22.

19. **Samuel BS1, Hansen EE, Manchester JK, Coutinho PM, Henrissat B, Fulton R, Latreille P, Kim K, Wilson RK, Gordon JI.** 2007**.** Genomic and metabolic adaptations of Methanobrevibacter smithii to the human gut. Proc Natl Acad Sci U S A. **104**:10643-8.

20. **Kates, M., M. K. Wassef, and E. L. Pugh.** 1970. Origin of the glycerol moieties in the glycerol diether lipids of *Halobacterium cutirubrum*. Biochim Biophys Acta **202:**206-8.

21. **Koga, Y., and H. Morii.** 2007. Biosynthesis of ether-type polar lipids in archaea and evolutionary considerations. Microbiol Mol Biol Rev **71:**97-120.

22. **Zhang, D.-L., L. Daniels, and C. D. Poulter**. 1990. Biosynthesis of archaebacterial membranes. Formation of isoprene ethers by a prenyl transfer reaction. J. Am. Chem. Soc. **112**:1264-1265

23. **Chen, A., and C. D. Poulter.** 1993. Purification and characterization of farnesyl diphosphate/geranylgeranyl diphosphate synthase. A thermostable bifunctional enzyme from *Methanobacterium thermoautotrophicum*. J Biol Chem **268:**11002-7.

24. **Koga, Y.** 2012. Thermal adaptation of the archaeal and bacterial lipid membranes. Archaea **2012:**789652.

25. **de Rosa, M. d. R., S. Gambacorta, L. Minale, L. Bu'lockb, J.** 1977. Chemical structure of the ether lipids of thermophilic acidophilic bacteria of the Caldariella group. Phytochemistry **16:**1961–1965.

26. **Miziorko, H. M.** 2010. Enzymes of the mevalonate pathway of isoprenoid biosynthesis. Arch Biochem Biophys **505:**131-43.

27. **Hunter, W. N.** 2007. The non-mevalonate pathway of isoprenoid precursor biosynthesis. J Biol Chem **282:**21573-7.

28. **Ekiel, I., I. C. Smith, and G. D. Sprott.** 1983. Biosynthetic pathways in *Methanospirillum hungatei* as determined by 13C nuclear magnetic resonance. J Bacteriol **156:**316-26.

29. **Ekiel, I., G. D. Sprott, and G. B. Patel.** 1985. Acetate and CO2 assimilation by *Methanothrix concilii*. J Bacteriol **162:**905-8.

30. **Ekiel, I., G. D. Sprott, and I. C. Smith.** 1986. Mevalonic acid is partially synthesized from amino acids in *Halobacterium cutirubrum*: a 13C nuclear magnetic resonance study. J Bacteriol **166:**559-64.

31. **Bult, C. J., O. White, G. J. Olsen, L. Zhou, R. D. Fleischmann, G. G. Sutton, J. A. Blake, L. M. FitzGerald, R. A. Clayton, J. D. Gocayne, A. R. Kerlavage, B. A. Dougherty, J. F. Tomb, M. D. Adams, C. I. Reich, R. Overbeek, E. F. Kirkness, K. G. Weinstock, J. M. Merrick, A. Glodek, J. L. Scott, N. S. Geoghagen, and J. C. Venter.** 1996. Complete genome sequence of the methanogenic archaeon*, Methanococcus jannaschii*. Science **273:**1058-73.

32. **Bochar, D. A., J. R. Brown, W. F. Doolittle, H. P. Klenk, W. Lam, M. E. Schenk, C. V. Stauffacher, and V. W. Rodwell.** 1997. 3-hydroxy-3-methylglutaryl coenzyme A reductase of *Sulfolobus solfataricus:* DNA sequence, phylogeny, expression in

Escherichia coli of the hmgA gene, and purification and kinetic characterization of the gene product. J Bacteriol **179:**3632-8.

33. **Bischoff, K. M., and V. W. Rodwell.** 1996. 3-Hydroxy-3-methylglutaryl-coenzyme A reductase from *Haloferax volcanii*: purification, characterization, and expression in *Escherichia coli*. J Bacteriol **178:**19-23.
34. **Kim, D. Y., C. V. Stauffacher, and V. W. Rodwell.** 2000. Dual coenzyme specificity of *Archaeoglobus fulgidus* HMG-CoA reductase. Protein Sci **9:**1226-34.
35. **Matsumi, R., H. Atomi, A. J. Driessen, and J. van der Oost.** 2011. Isoprenoid biosynthesis in Archaea--biochemical and evolutionary implications. Res Microbiol **162:**39-52.
36. **Lombard, J., and D. Moreira.** 2010. Origins and early evolution of the mevalonate pathway of isoprenoid biosynthesis in the three domains of life. Mol Biol Evol **28:**87-99.
37. **Huang, K. X., A. I. Scott, and G. N. Bennett.** 1999. Overexpression, purification, and characterization of the thermostable mevalonate kinase from *Methanococcus jannaschii*. Protein Expr Purif **17:**33-40.
38. **Primak, Y. A., M. Du, M. C. Miller, D. H. Wells, A. T. Nielsen, W. Weyler, and Z. Q. Beck.** 2011. Characterization of a feedback-resistant mevalonate kinase from the archaeon *Methanosarcina mazei*. Appl Environ Microbiol **77:**7772-8.
39. **Zhuang, N., K. H. Seo, C. Chen, J. Zhou, S. W. Kim, and K. H. Lee.** 2012. Crystallization and preliminary X-ray diffraction analysis of mevalonate kinase from *Methanosarcina mazei*. Acta Crystallogr Sect F Struct Biol Cryst Commun **68:**1560-3.

40. **Fu, Z., N. E. Voynova, T. J. Herdendorf, H. M. Miziorko, and J. J. Kim.** 2008. Biochemical and structural basis for feedback inhibition of mevalonate kinase and isoprenoid metabolism. Biochemistry **47:**3715-24.

41. **Voynova, N. E., S. E. Rios, and H. M. Miziorko.** 2004. *Staphylococcus aureus* mevalonate kinase: isolation and characterization of an enzyme of the isoprenoid biosynthetic pathway. J Bacteriol **186:**61-7.

42. **Andreassi, J. L., 2nd, P. W. Bilder, M. W. Vetting, S. L. Roderick, and T. S. Leyh.** 2007. Crystal structure of the *Streptococcus pneumoniae* mevalonate kinase in complex with diphosphomevalonate. Protein Sci **16:**983-9.

43. **Gray, J. C., and R. G. Kekwick.** 1972. The inhibition of plant mevalonate kinase preparations by prenyl pyrophosphates. Biochim Biophys Acta **279:**290-6.

44. **Tchen, T. T.** 1958. Mevalonic kinase: purification and properties. J Biol Chem **233:**1100-3.

45. **Barkley, S. J., R. M. Cornish, and C. D. Poulter.** 2004. Identification of an Archaeal type II isopentenyl diphosphate isomerase in *Methanothermobacter thermautotrophicus*. J Bacteriol **186:**1811-7.

46. **Siddiqui, M. A., A. Yamanaka, K. Hirooka, T. Bamaba, A. Kobayashi, T. Imanaka, E. Fukusaki, and S. Fujiwara.** 2005. Enzymatic and structural characterization of type II isopentenyl diphosphate isomerase from hyperthermophilic archaeon *Thermococcus kodakaraensis*. Biochem Biophys Res Commun **331:**1127-36.

47. **Hoshino, T., E. Nango, S. Baba, T. Eguchi, and T. Kumasaka.** 2010. Crystallization and preliminary X-ray analysis of isopentenyl diphosphate isomerase from

Methanocaldococcus jannaschii. Acta Crystallogr Sect F Struct Biol Cryst Commun **67:**101-3.

48. **Nakatani, H., S. Goda, H. Unno, T. Nagai, T. Yoshimura, and H. Hemmi.** 2012. Substrate-induced change in the quaternary structure of type 2 isopentenyl diphosphate isomerase from *Sulfolobus shibatae*. J Bacteriol **194:**3216-24.
49. **Nishimura, H., Y. Azami, M. Miyagawa, C. Hashimoto, T. Yoshimura, and H. Hemmi.** 2013. Biochemical evidence supporting the presence of the classical mevalonate pathway in the thermoacidophilic archaeon *Sulfolobus solfataricus*. J Biochem **153:**415-20.
50. **Boucher, Y., M. Kamekura, and W. F. Doolittle.** 2004. Origins and evolution of isoprenoid lipid biosynthesis in archaea. Mol Microbiol **52:**515-27.
51. **Grochowski, L. L., H. Xu, and R. H. White.** 2006. *Methanocaldococcus jannaschii* uses a modified mevalonate pathway for biosynthesis of isopentenyl diphosphate. J Bacteriol **188:**3192-8.
52. **Dellas, N., and J. P. Noel.** 2010. Mutation of archaeal isopentenyl phosphate kinase highlights mechanism and guides phosphorylation of additional isoprenoid monophosphates. ACS Chem Biol **5:**589-601.
53. **Chen, M., and C. D. Poulter.** 2010. Characterization of thermophilic archaeal isopentenyl phosphate kinases. Biochemistry **49:**207-17.
54. **Mabanglo, M. F., H. L. Schubert, M. Chen, C. P. Hill, and C. D. Poulter.** 2010. X-ray structures of isopentenyl phosphate kinase. ACS Chem Biol **5:**517-27.

55. **Allers, T.** 2010. Overexpression and purification of halophilic proteins in *Haloferax volcanii*. Bioeng Bugs **1:**288-90.

56. **Allers, T., S. Barak, S. Liddell, K. Wardell, and M. Mevarech.** 2010. Improved strains and plasmid vectors for conditional overexpression of His-tagged proteins in *Haloferax volcanii*. Appl Environ Microbiol **76:**1759-69.

57. **Allers, T., H. P. Ngo, M. Mevarech, and R. G. Lloyd.** 2004. Development of additional selectable markers for the halophilic archaeon *Haloferax volcanii* based on the leuB and trpA genes. Appl Environ Microbiol **70:**943-53.

58. **Simon, E. S., D.** 1953. The preparation of S-succinyl coenzyme A. Am. Chem. Soc. **75**:2520.

59. **Wang, C. Z., and H. M. Miziorko.** 2003. Methodology for synthesis and isolation of 5-phosphomevalonic acid. Anal Biochem **321:**272-5.

60. **Reardon, J. E., and R. H. Abeles.** 1987. Inhibition of cholesterol biosynthesis by fluorinated mevalonate analogues. Biochemistry **26:**4717-22.

61. **Voynova, N. E., Z. Fu, K. P. Battaile, T. J. Herdendorf, J. J. Kim, and H. M. Miziorko.** 2008. Human mevalonate diphosphate decarboxylase: characterization, investigation of the mevalonate diphosphate binding site, and crystal structure. Arch Biochem Biophys **480:**58-67.

62. **Skaff, D., and H. M. Miziorko.** 2010. A visible wavelength spectrophotometric assay suitable for high-throughput screening of 3-hydroxy-3-methylglutaryl-CoA synthase. Anal Biochem **396:**96-102.

63. **Skaff, D. A., K. X. Ramyar, W. J. McWhorter, M. L. Barta, B. V. Geisbrecht, and H. M. Miziorko.** 2012. Biochemical and structural basis for inhibition of Enterococcus faecalis hydroxymethylglutaryl-CoA synthase, mvaS, by hymeglusin. Biochemistry **51:**4713-22.

64. **VanNice, J. C., D. A. Skaff, G. J. Wyckoff, and H. M. Miziorko.** 2013. Expression *in Haloferax volcanii* of 3-hydroxy-3-methylglutaryl coenzyme A synthase facilitates isolation and characterization of the active form of a key enzyme required for polyisoprenoid cell membrane biosynthesis in halophilic archaea. J Bacteriol **195:**3854-62.

65. **Ferguson, J. J., Jr., and H. Rudney.** 1959. The biosynthesis of beta-hydroxy-beta-methylglutaryl coenzyme A in yeast. I. Identification and purification of the hydroxymethylglutaryl coenzymecondensing enzyme. J Biol Chem **234:**1072-5.

66. **Rokosz, L. L., D. A. Boulton, E. A. Butkiewicz, G. Sanyal, M. A. Cueto, P. A. Lachance, and J. D. Hermes.** 1994. Human cytoplasmic 3-hydroxy-3-methylglutaryl coenzyme A synthase: expression, purification, and characterization of recombinant wild-type and Cys129 mutant enzymes. Arch Biochem Biophys **312:**1-13.

67. **Campobasso, N., M. Patel, I. E. Wilding, H. Kallender, M. Rosenberg, and M. N. Gwynn.** 2004. Staphylococcus aureus 3-hydroxy-3-methylglutaryl-CoA synthase: crystal structure and mechanism. J Biol Chem **279:**44883-8.

68. **Wilding, E. I., J. R. Brown, A. P. Bryant, A. F. Chalker, D. J. Holmes, K. A. Ingraham, S. Iordanescu, C. Y. So, M. Rosenberg, and M. N. Gwynn.** 2000. Identification,

evolution, and essentiality of the mevalonate pathway for isopentenyl diphosphate biosynthesis in gram-positive cocci. J Bacteriol **182:**4319-27.

69. **Servouse, M., N. Mons, J. L. Baillargeat, and F. Karst.** 1984. Isolation and characterization of yeast mutants blocked in mevalonic acid formation. Biochem Biophys Res Commun **123:**424-30.
70. **Timpson, L. M., A. K. Liliensiek, D. Alsafadi, J. Cassidy, M. A. Sharkey, S. Liddell, T. Allers, and F. Paradisi.** 2013. A comparison of two novel alcohol dehydrogenase enzymes (ADH1 and ADH2) from the extreme halophile Haloferax volcanii. Appl Microbiol Biotechnol **97:**195-203.
71. **Miziorko, H. M., and M. D. Lane.** 1977. 3-Hydroxy-3-methylgutaryl-CoA synthase. Participation of acetyl-S-enzyme and enzyme-S-hydroxymethylgutaryl-SCoA intermediates in the reaction. J Biol Chem **252:**1414-20.
72. **Misra, I., C. Narasimhan, and H. M. Miziorko.** 1993. Avian 3-hydroxy-3-methylglutaryl-CoA synthase. Characterization of a recombinant cholesterogenic isozyme and demonstration of the requirement for a sulfhydryl functionality in formation of the acetyl-enzyme reaction intermediate. J Biol Chem **268:**12129-35.
73. **Misra, I., and H. M. Miziorko.** 1996. Evidence for the interaction of avian 3-hydroxy-3-methylglutaryl-CoA synthase histidine 264 with acetoacetyl-CoA. Biochemistry **35:**9610-6.
74. **Theisen, M. J., I. Misra, D. Saadat, N. Campobasso, H. M. Miziorko, and D. H. Harrison.** 2004. 3-hydroxy-3-methylglutaryl-CoA synthase intermediate complex observed in "real-time". Proc Natl Acad Sci U S A **101:**16442-7.

75. **Hartman, A. L., C. Norais, J. H. Badger, S. Delmas, S. Haldenby, R. Madupu, J. Robinson, H. Khouri, Q. Ren, T. M. Lowe, J. Maupin-Furlow, M. Pohlschroder, C. Daniels, F. Pfeiffer, T. Allers, and J. A. Eisen.** 2010. The complete genome sequence of *Haloferax volcanii* DS2, a model archaeon. PLoS One **5:**e9605.

76. **Madern, D., C. Ebel, and G. Zaccai.** 2000. Halophilic adaptation of enzymes. Extremophiles **4:**91-8.

77. **Sutherlin, A., M. Hedl, B. Sanchez-Neri, J. W. Burgner, 2nd, C. V. Stauffacher, and V. W. Rodwell.** 2002. *Enterococcus faecalis* 3-hydroxy-3-methylglutaryl coenzyme A synthase, an enzyme of isopentenyl diphosphate biosynthesis. J Bacteriol **184:**4065-70.

78. **Clinkenbeard KD, Sugiyama T, Lane MD**. 1975. Cytosolic 3-hydroxy-3-methylglutaryl-CoA synthase from chicken liver. Methods Enzymol. **35**:160–167.

79. **Tomoda, H., H. Kumagai, Y. Takahashi, Y. Tanaka, Y. Iwai, and S. Omura.** 1988. F-244 (1233A), a specific inhibitor of 3-hydroxy-3-methylglutaryl coenzyme A synthase: taxonomy of producing strain, fermentation, isolation and biological properties. J Antibiot (Tokyo) **41:**247-9.

80. **Middleton, B**. 1972. The kinetic mechanism of 3-hydroxy-3-methylglutaryl-coenzyme A synthase from baker's yeast. Biochem. J. **126**:35–47.

81. **Greenspan, M. D., H. G. Bull, J. B. Yudkovitz, D. P. Hanf, and A. W. Alberts.** 1993. Inhibition of 3-hydroxy-3-methylglutaryl-CoA synthase and cholesterol biosynthesis by beta-lactone inhibitors and binding of these inhibitors to the enzyme. Biochem J. **289:**889-95.

82. **Hellig, H. Popjak, J**. 1961.Studies on the biosynthesis of cholesterol: XIII. phosphomevalonic kinase from liver. J. Lipid Research. **2**:235-243.

83. **Herdendorf, T. J., and H. M. Miziorko.** 2006. Phosphomevalonate kinase: functional investigation of the recombinant human enzyme. Biochemistry **45:**3235-42.

84. **Bazaes S, Beytía E, Jabalquinto AM, Solís de Ovando F, Gómez I, Eyzaguirre J**. 1980. Pig liver phosphomevalone kinase. 1. Purification and properties. Biochemistry. **11**:2300-4.

85. **Alvear M, Jabalquinto AM, Eyzaguirre J, Cardemil E**. 1982. Purification and characterization of avian liver mevalonate-5-pyrophosphate decarboxylase. Biochemistry. **21**:4646-50.

86. **Byres, E., M. S. Alphey, T. K. Smith, and W. N. Hunter.** 2007. Crystal structures of *Trypanosoma brucei* and *Staphylococcus aureus* mevalonate diphosphate decarboxylase inform on the determinants of specificity and reactivity. J Mol Biol **371:**540-53.

87. **Pilloff, D., K. Dabovic, M. J. Romanowski, J. B. Bonanno, M. Doherty, S. K. Burley, and T. S. Leyh.** 2003. The kinetic mechanism of phosphomevalonate kinase. J Biol Chem **278:**4510-5.

88. **Doun, S. S., J. W. Burgner, 2nd, S. D. Briggs, and V. W. Rodwell.** 2005. *Enterococcus faecalis* phosphomevalonate kinase. Protein Sci **14:**1134-9.

89. **Romanowski, M. J., J. B. Bonanno, and S. K. Burley.** 2002. Crystal structure of the *Streptococcus pneumoniae* phosphomevalonate kinase, a member of the GHMP kinase superfamily. Proteins **47:**568-71.

90. **Barta, M. L., D. A. Skaff, W. J. McWhorter, T. J. Herdendorf, H. M. Miziorko, and B. V. Geisbrecht.** 2011. Crystal structures of *Staphylococcus epidermidis* mevalonate diphosphate decarboxylase bound to inhibitory analogs reveal new insight into substrate binding and catalysis. J Biol Chem **286:**23900-10.

91. **Dhe-Paganon, S., J. Magrath, and R. H. Abeles.** 1994. Mechanism of mevalonate pyrophosphate decarboxylase: evidence for a carbocationic transition state. Biochemistry **33:**13355-62.

92. **Reardon, J. E., and R. H. Abeles.** 1987. Inhibition of cholesterol biosynthesis by fluorinated mevalonate analogues. Biochemistry **26:**4717-22.

93. **Krepkiy, D., and H. M. Miziorko.** 2004. Identification of active site residues in mevalonate diphosphate decarboxylase: implications for a family of phosphotransferases. Protein Sci **13:**1875-81.

94. **Krepkiy, D. V., and H. M. Miziorko.** 2005. Investigation of the functional contributions of invariant serine residues in yeast mevalonate diphosphate decarboxylase. Biochemistry **44:**2671-7.

95. **VanNice, J. C., D. A. Skaff, G. J. Wyckoff, and H. M. Miziorko.** 2014. Identification in *Haloferax volcanii* of Phosphomevalonate Decarboxylase and Isopentenyl Phosphate Kinase as Catalysts of the Terminal Enzyme Reactions in an Archaeal Alternate Mevalonate Pathway. J Bacteriol **196:** 1055-63.

96. **Chang Q, Yan XX, Gu SY, Liu JF, Liang DC**. 2008. Crystal structure of human phosphomevalonate kinase at 1.8 A resolution. Proteins. **1**: 254-8.

97. **Herdendorf TJ, Miziorko HM.** 2006. Phosphomevalonate kinase: functional investigation of the recombinant human enzyme. Biochemistry. **10**: 3235-42.

VITA

John was born in 1979 in Fort Scott, Kansas. After graduating high school, John attended the University of Kansas, Lawrence graduating with a Bachelor's degree in Biochemistry and Microbiology. He took a position with Johns Manville designing new products. During his time at JM, he was awarded a patent (US #7967905). John then returned to graduate school to obtain a master's degree in molecular biology from the University of Missouri – Kansas City. He then decided to stay and complete his doctorate. His dissertation work resulted in two first author publications (64, 95).